2003

A Comparison of Pole Assignment & LQR Design Methods for Multivariable Control for Statcom

Liqun Xing

THE FLORIDA STATE UNIVERSITY

COLLEGE OF ENGINEERING

A Comparison of Pole Assignment & LQR Design Methods for Multivariable Control for STATCOM

BY

LIQUN XING

A Thesis submitted to the
Department of Mechanical Engineering
In partial fulfillment of the
requirements for the degree of
Master of Science

Degree Awarded:
Fall Semester, 2003

ACKNOWLEGEMENTS

I would like to express my thanks and appreciation to my advisor, Dr. David Cartes for his continuous encouragement and kind help in my research and study. I am grateful to Dr. Emmanuel G.Collins and Dr. Rodney Roberts for their knowledge and guides in control theory. I also wish to thank Dr. Hui Li for her help in power electronics.

I would like to express my love and gratitude to my family for their support, patients, kindness, inspiration and love.

TABLE OF CONTENTS

LIST OF FIGURES

ABSTRACT

The static synchronous compensator (STATCOM) is increasingly popular in power system application. In general, power factor and stability of the utility system can be improved by STATCOM. Specifically, STATCOM can stabilize a given node voltage and compensate for the power factors of equipment serviced by that node. The dynamic performance of STATCOM is critical to these performance and stability function. STATCOM is a multiple input and multiple output system (MIMO), which can be presented by a mathematic model. Recently, full MIMO state feedback by pole assignment has been shown to be an improvement over classical PI control. In this thesis, an optimal linear quadratic regulator (LQR) design is a compared to the pole assignment design for transient dynamic performance of STATCOM. It was found that LQR controllers do not offer significant performance improvement to pole assignment. However, as a design method the determination of state feedback gains is easier using the LQR method

CHAPTER 1

INTRODUCTION

1.1 STATCOM Overview

In a direct current (DC) circuit, or in an alternating current (AC) circuit whose impedance is a pure resistance, the voltage and current are in phase, and the following formula holds:

$$P = E_{rms} * I_{rms}$$

Where P is the power in watts, E_{rms} is the root mean square (rms) voltage in watts, and I_{rms} is the rms current in amperes. But in an AC circuit whose impedance consists of reactance as well as resistance, the voltage and current are not in phase. This complicates the determination of power. In the absence of reactance, the product $E_{rms} * I_{rms}$ represents true power because it is manifested in tangible form (radiation, dissipation, and/or mechanical motion). But when there is reactance in an AC circuit, the product $E_{rms} * I_{rms}$ is greater than the true power. The excess is called reactive power, and represents energy alternately stored and released by inductors and/or capacitors. Reactive power affects system voltages, energy loss as well as system security.

In the control of electric power systems, reactive power compensation is an important issue. Reactive power increases transmission system losses, reduces power transmission capabilities, and may cause large amplitude variations in the receiving-end voltages. Moreover, rapid changes in reactive power consumption may lead to terminal voltage-amplitude oscillations. These voltage variations, which are caused by fluctuating reactive

power, can change the real power demand in the power system, resulting in power oscillations.

Reactive power compensation is traditionally realized by connecting or disconnecting capacitor or inductor banks to the bus through mechanical switches that are slow and imprecise. Over the last two decades, reactive power compensators based on force- commutated solid state power electronic devices, such as Thyristor-controlled Reactors (TCR) and Thyristor-switched Capacitor, have gained popularity. In these devices the effective reactance connected to the system is controlled by the fire angle of thyristors. These devices improved the dynamics and precision. However, they strongly depended on the power system line condition at the point–of-common-coupling voltage. Therefore they are very good steady state solution, but frequently exhibit poor transient dynamics. With the developments in power electronics, a new kind of compensator was introduced. This compensator is static synchronous compensator - STATCOM, which is based on self-commutated solid state power electronic devices to achieve advanced reactive power control. STATCOM is capable of high dynamic performance and its compensation does not depend on the common coupling voltage. Therefore, STATCOM is very effective during
the power system disturbances.

Moreover, much research confirms several advantages of STATCOM [1]-[3]. These advantages include:

- Size, weight, and cost reduction
- Equality of lagging and leading output
- Precise and continuous reactive power control with fast response
- Possible active harmonic filter capability

In 1991, the first STATCOM scaled model (80 MVAR) was designed and built at the Westinghouse Science and Technology Center, which proved that STATCOM can increase system damping, power system stabilization, and power transmission limits. In 1995 the first high power STATCOM in the United States (100 MVAR) was commissioned at the Sullivan substation of the Tennessee Valley Authority (TVA) for transmission line compensation. The project was jointly sponsored by the Electric Research Institute and TVA, and designed and manufactured by the Westinghouse

Electric Corporation. This project showed that the STATCOM is a versatile piece of equipment, with outstanding dynamic capability, that will find increased application in power systems. In 1996, the National Grid Company of England and Wales decided to design a dynamic reactive compensation equipment with inclusion of a STATCOM of 150 MVR range.

Confidence in the STATCOM principle has now grown sufficiently for some utilities to consider them for normal commercial service. Japan (Nagoya), United States, England and Australia (QLD) also use STATCOM in practice.

1.2. STATCOM Control

STATCOM is playing increasingly important roles in reactive power provision and voltage support because of its attractive steady state performance and operating characteristics, which have been well studied in past years [3, 4]. Much work about STATCOM steady state performance control has been done, which is based on the steady state vector (phasor) diagram analysis to power system quantities [5, 6]. This kind of control approach, usually a proportional integrated control (PI control), is convenient to the traditional power system analysis method and not necessary to build a special mathematic model for controller design. However, the system response is slow due to the calculation of active and reactive power, that need several periods (T) of the power system, and not effective when the change of power system is rapid [7].

As power system becomes more complex and more nonlinear loads are connected, the control of power system transient response is becoming a very critical issue. Therefore, it is necessary to study STATCOM dynamic characteristics and capabilities to improve transient stability. Analyses of STATCOM dynamic performance and control methods have been studied in recent years [8, 9]. The STATCOM control algorithm is based on the dynamic model rather than the phasor diagram. The calculation of active and reactive power based on frequency domain is not necessary for controlling STATCOM dynamic performance. In fact, the instantaneous values of power system parameters are used in STATCOM dynamic control, which means the response of STATCOM can be within one power system period.

The control algorithm to STATCOM dynamic performance depends on the dynamic model. Various dynamic models and control approaches have been applied to STATCOM dynamic control and have achieve many good results [10 -12]. Nevertheless, most of the work in literature has simplified the control efforts from multiple inputs by decoupling the state into several parallel single input systems, such that conventional PID control methods can be used. Some research focuses on forcing this assumption to be true in an inner loop [13].

1.3. Objectives and Motivation

It is desirable if we can utilize all the STATCOM dynamic characteristics and improve the dynamic performance of STATCOM further. In order to achieve this, we need to look at STATCOM as a real multiple input and multiple output system and avoid doing significant assumptions or approximations, which will compromise some of the STATCOM intrinsic and valuable characteristics.

Therefore, a STATCOM controller designed by using a multivariable control approach is needed. The dynamic mathematic model of STATCOM is the basis when deriving the control algorithm. We should analyze the STATCOM model first. There are different approaches for multivariable controller design. It is necessary to compare their performance for this special control issue. In this thesis, we compare pole assignment and optimal linear quadratic regulator in order to find which method is suitable for STATCOM.

In this thesis, first an overview of STATCOM and its control are given. Then we have analyzed a typical STATCOM circuit and find the mathematic model to represent its dynamic characteristics in chapter 2. Based on that model we will investigate STATCOM's open loop performance and its controllability in chapter 3. In chapter 4, we will first design controllers to get desired closed loop performances of STATCOM by using pole assignment and LQR methods. Then we will compare different control methods to find out which one is suitable for STATCOM. After designing and simulating our controller in Simulink we will run the circuit simulation to verify our design method in chapter 5.

CHAPTER 2

STATCOM MODELING

2.1. Circuit Model

The voltage source converter based STATCOM is the dominant topology in practice. Figure 2.1 is the circuit diagram of a typical STATCOM.

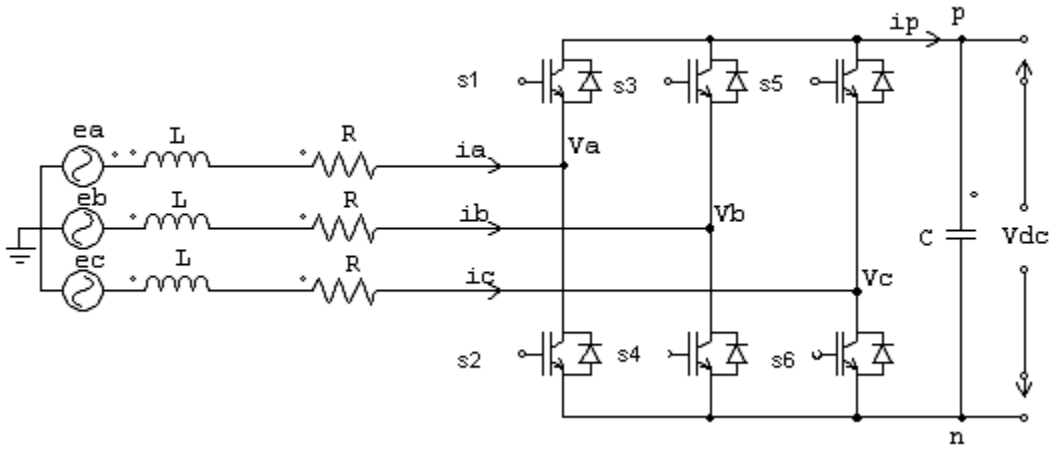

Figure 2.1. Equivalent circuit of STATCOM

Where

i_a, i_b, i_c	line current;
V_a, V_b, V_c	converter phase voltage;
e_a, e_b, e_c	AC source phase voltage;
$Vdc = Vpn$	DC side voltage;
i_p	DC side current;
L	inductance of the line reactor;
R	resistance of the line reactor;
C	DC side capacitor,

2.2. Mathematic Model

Based on the equivalent circuit of STATCOM shown in Figure 2.1 we can derive the mathematic model of STATCOM as fallow.

From power electronics principles we get

$$i_p = \begin{bmatrix} D_{ap} - D_{bp} \\ D_{bp} - D_{cp} \\ D_{cp} - D_{ap} \end{bmatrix}^T \begin{bmatrix} i_{ab} \\ i_{bc} \\ i_{ca} \end{bmatrix} \tag{2.1}$$

Where

D_{kp} are switching functions and $k = a, b, c$

$$i_{ab} = \frac{1}{3}(i_a - i_b),\ i_{bc} = \frac{1}{3}(i_b - i_c),\ i_{ca} = \frac{1}{3}(i_c - i_a)$$

and

$$\begin{bmatrix} V_a - V_b \\ V_b - V_c \\ V_c - V_a \end{bmatrix} = \begin{bmatrix} D_{ap} - D_{bp} \\ D_{pb} - D_{cp} \\ D_{cp} - D_{ap} \end{bmatrix} Vpn \quad . \tag{2.2}$$

From circuit principles we get

$$Ri_a + L\frac{di_a}{dt} = e_a - V_a \tag{2.3}$$

$$Ri_b + L\frac{di_b}{dt} = e_b - V_b \tag{2.4}$$

$$Ri_c + L\frac{di_c}{dt} = e_c - V_c \tag{2.5}$$

and

$$L\frac{di_{ab}}{dt} = \frac{1}{3}L(\frac{di_a}{dt} - \frac{di_b}{dt}) \tag{2.6}$$

this equation can be expanded as below

$$\begin{aligned} L\frac{di_{ab}}{dt} &= \frac{1}{3}[(e_a - V_a) - (e_b - V_b)] - i_{ab}R \\ &= \frac{1}{3}[(e_a - e_b) - (V_a - V_b)] - i_{ab}R \end{aligned} \tag{2.7}$$

similarly we can get

$$L\frac{di_{bc}}{dt} = \frac{1}{3}[(e_b - e_c) - (V_b - V_c)] - i_{bc}R \tag{2.8}$$

$$L\frac{di_{ca}}{dt} = \frac{1}{3}[(e_c - e_a) - (V_c - V_a)] - i_{ca}R \tag{2.9}$$

putting equations (2.7), (2.8) and (2.9) together we have

$$\frac{d}{dt}\begin{bmatrix} i_{ab} \\ i_{bc} \\ i_{ca} \end{bmatrix} = \frac{1}{3L}\begin{bmatrix} e_a - e_b \\ e_b - e_c \\ e_c - e_a \end{bmatrix} - \frac{1}{3L}\begin{bmatrix} V_a - V_b \\ V_b - V_c \\ V_c - V_a \end{bmatrix} - \frac{R}{L}\begin{bmatrix} i_{ab} \\ i_{bc} \\ i_{ca} \end{bmatrix}. \tag{2.10}$$

By applying equation (2.2) to equation (2.10)

$$\frac{d}{dt}\begin{bmatrix} i_{ab} \\ i_{bc} \\ i_{ca} \end{bmatrix} = \frac{1}{3L}\begin{bmatrix} e_a - e_b \\ e_b - e_c \\ e_c - e_a \end{bmatrix} - \frac{1}{3L}\begin{bmatrix} D_{ap} - D_{bp} \\ D_{pb} - D_{cp} \\ D_{cp} - D_{ap} \end{bmatrix} Vpn - \frac{R}{L}\begin{bmatrix} i_{ab} \\ i_{bc} \\ i_{ca} \end{bmatrix} \tag{2.11}$$

and

$$C\frac{dVpn}{dt} = i_p = \begin{bmatrix} D_{ap} - D_{bp} \\ D_{bp} - D_{cp} \\ D_{cp} - D_{ap} \end{bmatrix}^T \begin{bmatrix} i_{ab} \\ i_{bc} \\ i_{ca} \end{bmatrix}. \tag{2.12}$$

It is common practical in power system application to transform 3 phase AC dynamics into orthogonal components in a rotating reference frame. Here components are referred to as the real and reactive components, those that lead to useful work and those that do not respectively. From the power system theory we get the real and reactive currents relative to a rotating reference frame with angular frequency ω as

$$\begin{bmatrix} i_d \\ i_q \\ 0 \end{bmatrix} = P\begin{bmatrix} i_a \\ i_b \\ i_c \end{bmatrix} \tag{2.13}$$

and

$$P = \frac{2}{3}\begin{bmatrix} \cos(\omega t) & \cos(\omega t - \frac{2}{3}\pi) & \cos(\omega t + \frac{2}{3}\pi) \\ -\sin(\omega t) & -\sin(\omega t - \frac{2}{3}\pi) & -\sin(\omega t + \frac{2}{3}\pi) \\ \frac{1}{2} & \frac{1}{2} & \frac{1}{2} \end{bmatrix} \tag{2.14}$$

where

i_d active current component,

i_q reactive current component,

then we have

$$\begin{bmatrix} i_{ab} \\ i_{bc} \\ i_{ca} \end{bmatrix} = \frac{1}{3}\begin{bmatrix} i_a - i_b \\ i_b - i_c \\ i_c - i_a \end{bmatrix} = \frac{1}{3}\left(\begin{bmatrix} i_a \\ i_b \\ i_c \end{bmatrix} - \begin{bmatrix} i_b \\ i_c \\ i_a \end{bmatrix}\right) = \overline{T}^{-1}\begin{bmatrix} i_d \\ i_q \\ 0 \end{bmatrix} \tag{2.15}$$

where

$$\overline{T}^{-1} = \frac{1}{\sqrt{3}}\begin{bmatrix} -\sin(\omega t - \frac{1}{3}\pi) & \cos(\omega t - \frac{1}{3}\pi) & 1 \\ \sin(\omega t) & -\cos(\omega t) & 1 \\ -\sin(\omega t + \frac{1}{3}\pi) & \cos(\omega t + \frac{1}{3}\pi) & 1 \end{bmatrix} \tag{2.16}$$

if we set T as the first two 2×3 subspace of matrix $\overline{T}$, we can get

$$\begin{bmatrix} i_d \\ i_q \end{bmatrix} = T\begin{bmatrix} i_{ab} \\ i_{bc} \\ i_{ca} \end{bmatrix} \tag{2.17}$$

similarly we can get

$$\begin{bmatrix} e_d \\ e_q \end{bmatrix} = T \begin{bmatrix} e_{ab} \\ e_{bc} \\ e_{ca} \end{bmatrix} \tag{2.18}$$

$$\begin{bmatrix} D_d \\ D_q \end{bmatrix} = T \begin{bmatrix} D_{ab} \\ D_{bc} \\ D_{ca} \end{bmatrix} \tag{2.19}$$

applying equation (2.17) to the left part of equation (2.11)

$$\frac{d}{dt}\begin{bmatrix} i_{ab} \\ i_{bc} \\ i_{ca} \end{bmatrix} = \frac{d(T^{-1}\begin{bmatrix} i_d \\ i_q \end{bmatrix})}{dt} = \frac{dT^{-1}}{dt}\begin{bmatrix} i_d \\ i_q \end{bmatrix} + T^{-1}\begin{bmatrix} \frac{di_d}{dt} \\ \frac{di_q}{dt} \end{bmatrix} \tag{2.20}$$

applying equations (2.18) and (2.19) to equation (2.11)

$$\frac{dT^{-1}}{dt}\begin{bmatrix} i_d \\ i_q \end{bmatrix} + T^{-1}\begin{bmatrix} \frac{di_d}{dt} \\ \frac{di_q}{dt} \end{bmatrix} = \frac{1}{3L}T^{-1}\begin{bmatrix} e_d \\ e_q \end{bmatrix} - \frac{1}{3L}T^{-1}\begin{bmatrix} D_d \\ D_q \end{bmatrix} \cdot V_{pn} - \frac{R}{L}T^{-1}\begin{bmatrix} i_d \\ i_q \end{bmatrix}. \tag{2.21}$$

From power system principles we get

$$e_d = V_m$$

$$e_q = 0$$

and

$$T\frac{dT^{-1}}{dt} = \begin{bmatrix} 0 & -\omega \\ \omega & 0 \end{bmatrix} \tag{2.22}$$

multiply T to both side of equation (2.21) and applying equation (2.22), we obtain

$$\begin{bmatrix} \frac{di_d}{dt} \\ \frac{di_q}{dt} \end{bmatrix} = \begin{bmatrix} -\frac{R}{L} & \omega & -\frac{Dd}{3L} \\ -\omega & -\frac{R}{L} & -\frac{Dq}{3L} \end{bmatrix} \begin{bmatrix} i_d \\ i_q \\ Vdc \end{bmatrix} + \begin{bmatrix} \frac{1}{3L} \\ 0 \\ 0 \end{bmatrix} V_m . \tag{2.22}$$

By applying equations (2.17) and (2.19) to equation (2.12) we have

$$\frac{dVdc}{dt} = \frac{1}{C} i_p = \frac{1}{C} \begin{bmatrix} D_{ap} - D_{bp} \\ D_{bp} - D_{cp} \\ D_{cp} - D_{ap} \end{bmatrix}^T \begin{bmatrix} i_{ab} \\ i_{bc} \\ i_{ca} \end{bmatrix} = \begin{bmatrix} D_d \\ D_q \end{bmatrix}^T T^{-T} T^{-1} \begin{bmatrix} i_d \\ i_q \end{bmatrix} = \frac{3}{2C} \begin{bmatrix} D_d \\ D_q \end{bmatrix}^T \begin{bmatrix} i_d \\ i_q \end{bmatrix}.$$

Which leads to

$$\frac{dVdc}{dt} = \frac{dVpn}{dt} = \frac{1}{C} i_p = \frac{3}{2C} \begin{bmatrix} D_d \\ D_q \end{bmatrix}^T \begin{bmatrix} i_d \\ i_q \end{bmatrix}. \tag{2.23}$$

Rearranging equations (2.22) and (2.23) we get

$$\frac{di_d}{dt} = \frac{-R}{L} i_d + i_q \omega - \frac{Vdc}{3L} D_d + \frac{1}{3L} V_m \tag{2.24}$$

$$\frac{di_q}{dt} = -i_d \omega - \frac{R}{L} i_q - \frac{Vdc}{3L} D_q \tag{2.25}$$

$$\frac{dVdc}{dt} = \frac{3}{2C} i_d D_d + \frac{3}{2C} i_q D_q \tag{2.26}$$

Finally we find that we can represent the "outer loop" dynamics of STATCOM, the dynamics resulting from any arbitrary switching function D_k, by representing equation (2.26) in its the standard state space form

$$\frac{d}{dt}\begin{bmatrix} i_d \\ i_q \\ Vdc \end{bmatrix} = \begin{bmatrix} -\frac{R}{L} & \omega & -\frac{D_d}{3L} \\ -\omega & -\frac{R}{L} & -\frac{D_q}{3L} \\ \frac{3}{2C}D_d & \frac{3}{2C}D_q & 0 \end{bmatrix} \begin{bmatrix} i_d \\ i_q \\ V_{dc} \end{bmatrix} + \begin{bmatrix} \frac{1}{3L} \\ 0 \\ 0 \end{bmatrix} V_m \qquad (2.27)$$

This completes the nonswitching dynamic model of STATCOM as equation (2.27). From the model we can see the states of the STATCOM dynamic loop are i_d, i_q and V_{dc}. V_m can be considered as a system constant parameter. The control variables are D_d, D_q. Note that this is a bilinear system and in our application, full state feedback control of STATCOM, represents a nonlinear system.

2.3. Operating Condition

In our application, we selected the circuit parameters, for the circuit shown in Fig. 2.1, and operating condition as below:

Circuit parameters;

$R = 0.02\Omega$; $L = 2.8e-03H$; $C = 0.1F$;

$V_m = 5882V$; ω=377 rad/s

Desired steady states:

Vdc =10000A

i_d =0 A;

i_q =178A;

Dd =0;

Dq =0.6445;

CHAPTER 3

ANALYSIS OF THE STATCOM MODEL

From the STATCOM mathematic model (2.27), we can see that it is a nonlinear system. The problem then is how we can deal with the nonlinear characteristics in the controlled STATCOM. There are different methods, which can be used to control a nonlinear system. Since we know the operating points of the STATCOM we can use the linearization method to cope with this nonlinear problem.

3.1 Linearization of STATCOM Model

Here we linearize using the method of Jacobian. By using Jacobian matrix method, we can linearize equation (2.27) to linear equations around a given operating point.

If $f(x)$ is the function to be linaerized and $f(x) \in \Re^{3\times 1}$ then this Jacobian can be

$$\frac{\partial f}{\partial x} = \begin{bmatrix} \frac{\partial f1}{\partial x1} & \frac{\partial f2}{\partial x1} & \frac{\partial f3}{\partial x1} \\ \frac{\partial f1}{\partial x2} & \frac{\partial f2}{\partial x2} & \frac{\partial f3}{\partial x2} \\ \frac{\partial f1}{\partial x3} & \frac{\partial f2}{\partial x3} & \frac{\partial f3}{\partial x3} \end{bmatrix} \qquad (3.1)$$

For a nonlinear system, we may express the dynamics in the general vector function form as $\dot{X} = f(x,u)$. However pole assignment and LQR methods require us to use a linear time invariant (LTI) presentation of the system as found in equation (3.2).

Because of the presence of nonlinear terms in the state equations, we need to linearize the nonlinear vector function around the operating points of x^0 and u^0 by using Jacobian matrixes A and B, as shown below:

$$\begin{aligned} \dot{x} &= Ax + Bu \\ y &= Cx \end{aligned} \tag{3.2}$$

$$A = \frac{\partial f}{\partial x}\Big| x^0, u^0 \tag{3.3}$$

$$B = \frac{\partial f}{\partial u}\Big| x^0, u^0 \tag{3.4}$$

If we set $x = x^0 + \delta x$ and $u = u^0 + \delta u$ as the states we can get the new linear system as below:

$$\delta \dot{x} = A\delta x + B\delta u\,. \tag{3.5}$$

This linearized model is of the standard LTI form.

For the STATCOM model, we can use this procedure to get the linearized model. First we set operating points as

$$X^0 = \begin{bmatrix} i_{d_0} \\ i_{q_0} \\ V_{dc_0} \end{bmatrix} \qquad U^0 = \begin{bmatrix} Dd_0 \\ Dq_0 \end{bmatrix} \tag{3.6}$$

Here compute the Jacobians

$$A = \frac{\partial f}{\partial x}\left|\left(x^0, u^0\right) = \begin{bmatrix} \frac{-R}{L} & \omega & \frac{-Dd_0}{3L} \\ -\omega & \frac{-R}{L} & \frac{-Dq_0}{3L} \\ \frac{3Dd_0}{2C} & \frac{3Dq_0}{2C} & 0 \end{bmatrix}\right. \tag{3.7}$$

and

$$B = \frac{\partial f}{\partial u}\left(x^0, u^0\right) = \begin{bmatrix} -\frac{V_{dc_0}}{3L} & 0 \\ 0 & -\frac{V_{dc_0}}{3L} \\ \frac{3i_{d0}}{2C} & \frac{3i_{q0}}{2C} \end{bmatrix} \tag{3.8}$$

C is the identity matrix and will be ignored in the remaining discussion.

If we set $\widetilde{X} = X - x^0$ and $\widetilde{U} = U - u^0$, we then get the small signal model of the STATCOM as below:

$$\dot{\widetilde{X}} = A\widetilde{X} + B\widetilde{U} \tag{3.9}$$

Since V_m is constant therefore it would not exist in small signal model given by (3.9).

3.2 Open loop characteristics of STATCOM Model

Having the linearized system state space model as equation (3.9), we can use the linear system method to analyze the characteristics of STATCOM model. There are several open loop system properties we need to know before we design the controller.

Although system observability and controllability are the properties of the system presentation, these are two important criterions that must be established before any attempt in controller design is done. These two characteristics of a system depend on the state space presentations of the system. For a given system, different state space presentations have different effects on the controller design algorithm.

Another important property of a system is its open loop dynamic response characteristic that gives us not only the background information about the system performance but also the guideline for controller design.

1. Obsevability and Controllability

The state space model of STATCOM has three state variables - i_q, i_d, V_{dc}. All of them can be measured from the power system, which means the system is observable.

However we only have two independent control inputs to the three system states, we need to see if the system is controllable. In our case, the state matrix $A \in \Re^{3\times 3}$ and the input matrix $B \in \Re^{3\times 2}$, We need to see if the system controllability matrix **Co** is full rank.

Where, **Co**= [A: AB : AAB]

From chapter 2.3 we know that given the follow component parameters

$R = 0.02\Omega$; $L = 2.8mH$;

$C = 0.1F$; $V_m = 5882V$; $\omega = 377 rad/s$

The operating point is

V_{dc} =10000A, i_d=0, i_q=178A;

Dd_0=0, Dq_0=0.6445;

Thus we get

$$A = \begin{bmatrix} -7.1429 & 377.0000 & 0 \\ -377.0000 & -7.1429 & 9.6675 \\ 0 & 9.6675 & 0 \end{bmatrix}$$

$$B = 1.0\text{e}+006 \times \begin{bmatrix} -1.1905 & 0 \\ 0 & -1.1905 \\ 0 & 0.0027 \end{bmatrix}$$

Thus Controllability matrix Co is

$$Co = 1.0\text{e}+010 \times \begin{bmatrix} 9.9252 & 0.0001 & -0.0000 \\ 0.0001 & 9.9165 & -0.0424 \\ -0.0000 & -0.0424 & 1.0420 \end{bmatrix}$$

det (Co) =1.0254e+032

The **Co** matrix has full rank, thus the linearized model is controllable. One topic of the future work may be to examine this controllability for arbitrary operating point to obtain a general knowledge of operating point controllability.

2. Eigenvalues and Dynamic Performance

The open loop linearized system's eigenvalues are:

$$\Lambda = \begin{bmatrix} -7.12 + 3.7798\mathrm{i} \\ -7.12 - 3.7798\mathrm{i} \\ -0.04 \end{bmatrix} \times 1.0\ \text{e-}02$$

Since all the eigenvalues of the system are on the left hand of the plane, the system is stable.

The open loop dynamic performances on the operating point as below, in which the input value is Dd_0=0, Dq_0=0.6445. In the open loop system response shown in Figure 3.1-3, there are large oscillations in i_d and i_q during 0-0.6sec and V_{dc} is not constant.

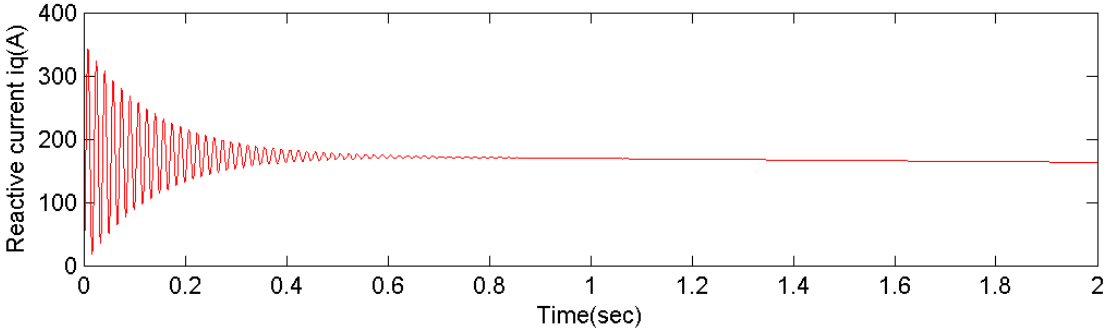

Figure 3.1 Open loop i_q response

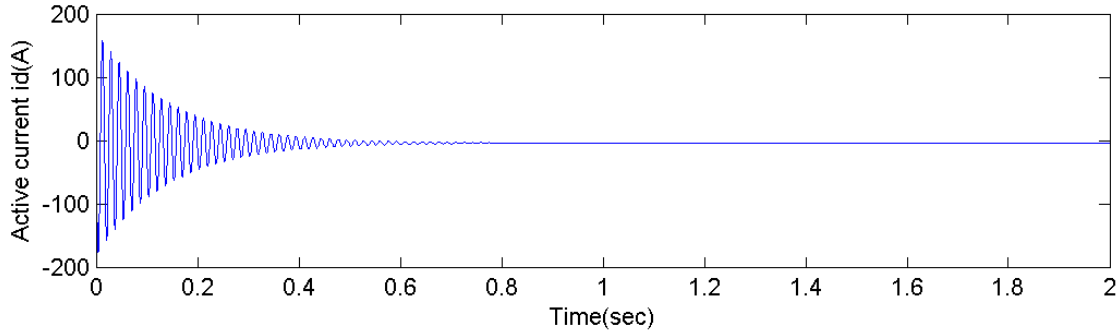

Figure 3.2 Open loop i_d response

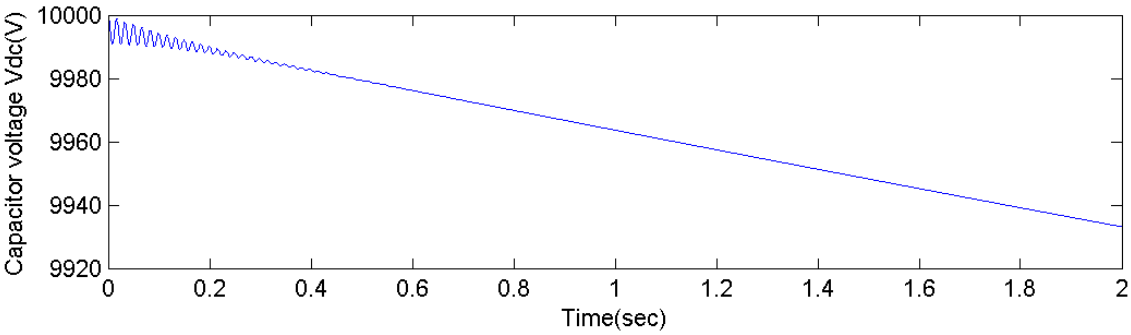

Figure 3.3 Open loop Vdc response

CHAPTER 4

MULTIVARIABLE CONTROLLER DESIGN

Since the STATCOM is used for instantaneous reactive power compensation for power systems, the i_q response should be within one period of the power system [5]. The frequency of the power system is 60 Hz, which means that one period is about 0.017sec. Thus the i_q transient response time should be less than 0.017sec. In the mean time the voltage of the capacitor V_{dc} should be kept constant [3]. The control effort of Dd and Dq should be within [-1, +1], see [17].

In the practice of STATCOM application, the operating point shift from the desired point. Thus another requirement for the controller is that the closed loop system should be robust enough to tolerate the minor change of the operating point and the potential change of the actual parameters of the STATCOM from those of the model.

There are several methods to implement this multivariable controller design. The first choice for this multivariable design is an attempt to find an approximate model through decoupling in which the controller design is decoupled into two or more single input –output models. This is the common practical solution for many STATCOM [10], [11], [12]. This method gives a simpler and more tractable subset of the system such that we can design the controller as in Single Input Single Output (SISO) application by using conventional PI control. However, decoupling this way leads to the STATCOM performance become very sensitive about its operating point, [13]. Thus we choose use other methods to design our controller that will be based on the coupled system model.

There are two main Multiple Input Multiple Output (MIMO) design methods: full state feedback design and LQR design. We will discuss these two methods used in STATCOM controller design.

4.1 Pole assignment controller design

A full state feedback controller based on the pole assignment method can improve the system characteristics such that the closed loop system performance will satisfy the requirement criteria.

4.1.1 Algorithm

For a given system:

$$\dot{x} = Ax + Bu; \tag{4.1}$$

Where,

$x \in \Re^N$ is the state vector

$u \in \Re^P$ is the input vector

$A \in \Re^{N \times N}$ is the basis matrix

$B \in \Re^{N \times P}$ is the input matrix

If we set controller as:

$$u(t) = -Kx(t). \tag{4.2}$$

Then the closed loop state equation can be obtained as

$$\dot{x}(t) = (A - BK)x(t). \tag{4.3}$$

This state equation describes the system formed by combining the plant and the controller. It is a homogeneous state equation, which has no input. The solution of this state is given by:

$$x(t) = e^{(A-BK)x(t)}x(0). \tag{4.4}$$

The state feedback controller $u(t) = -Kx(t)$ drives the state to zero for arbitrary initial conditions, provided that the closed loop poles ---the eigenvalues of $(A - BK)$--all

have negative real parts. By setting pole locations, we can make the closed loop system not only stable but also satisfy a given set of transient specifications.

A state feedback gain K that yields the closed loop poles $\{p1, p2, \cdots\cdots\cdots pn_x\}$ is obtained by solving the equation:

$$\det(sI - A + BK) = (s - p1)(s - p2)\cdots\cdots\cdots(s - pn_x). \qquad (4.5)$$

4.1.2 Eigenvalues Selection

The selection of closed loop system eigenvalues needs an understanding of the system characteristics and the limitation of the actuator. Different pole locations determine different system performance. This is the critical part of the controller design. By comparing the system performance in simulation, we can select the suitable pole locations as discussed in the following part.

4.1.3 Controller Design

We need a simulation loop to verify our controller performance before we validate it in the circuit loop, and we also need the simulation loop to help us design the controller. There are two tasks about the simulation: system loop and control loop. First, we need to build the open loop system simulation loop, which can represent the STATCOM dynamic performance. By using the STATCOM mathematic model, we get the system open loop model in Simulink as that is a representation of equation (2.27). With a loop, we can build the closed full state feedback loop as shown in Figure 4.1.

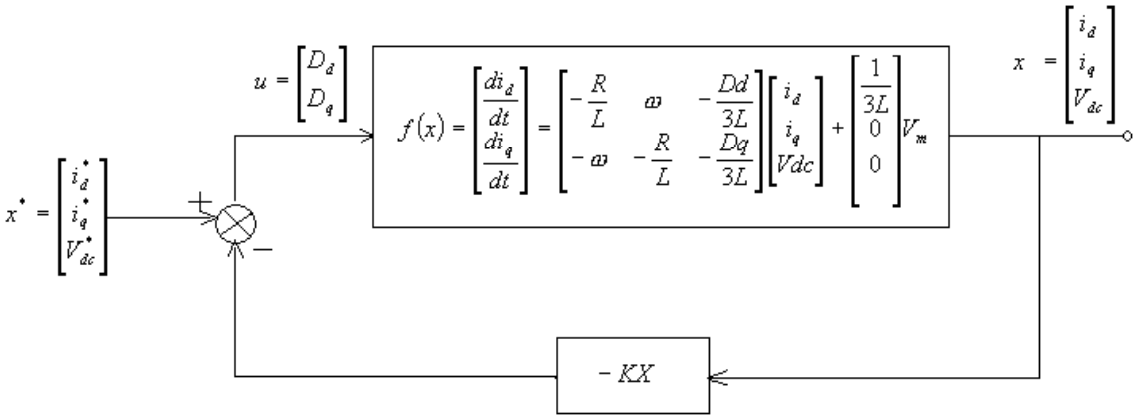

Figure 4.1 Closed loop control diagram

When we look at the open loop system response, Figure 3.1-3, we can find several dynamic characteristics need to be improved:

1. The eigenvalues of i_q and i_d are poorly damped.

2. The settling times of i_q and i_d (nearly 0.7sec) are larger than the requirement (less than 0.017sec).

3. The Overshoot of i_q and i_d is excessive.

4. The voltage of the capacitor V_{dc} does not remain around to a steady constant value 10000V.

In order to improve the dynamic characteristic above, we need to select the poles carefully and compromise different requirements. By this we mean the i_q transient response time should be less than 0.017sec. During that time the capacitor voltage V_{dc}, should be kept constant. Also, the control effort of Dd and Dq should be within [-1, +1].

First, we increase the real part value of the poles to add damping effect. In order to achieve that, the real part of the poles for i_q and i_d are increased by a factor of 240.45

and real part of V_{dc} pole is increased by a factor of 1000. The closed loop system response is shown in Figure 4.2-4.4. We can see that the settling time is about 0.3 sec in i_q and i_d response, which is much better than the open loop response. The settling time of V_{dc} decreases to around 0.3sec even though it still dose not converge to the constant value around 10000V. However, the overshoots of i_q, and i_d are larger than the open loop response.

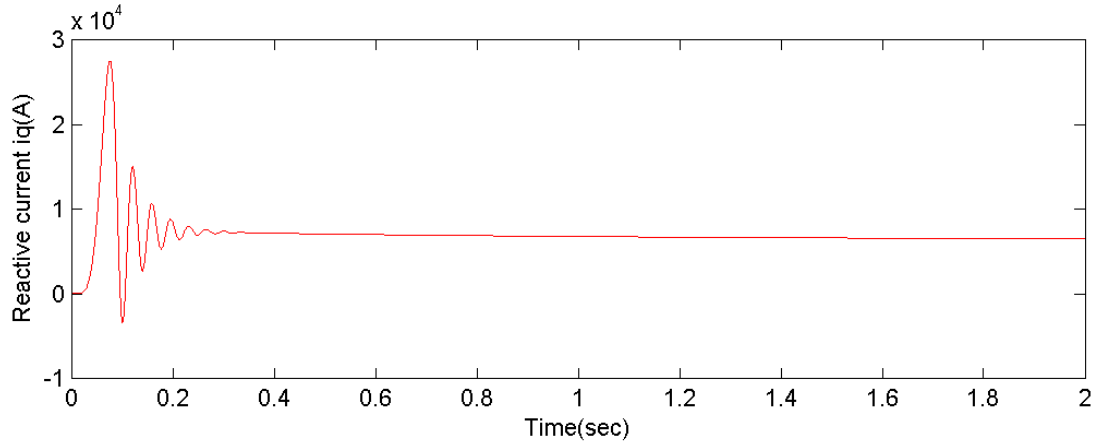

Figure 4.2 i_q response when poles in [-17.21 -17.21 -0.4]

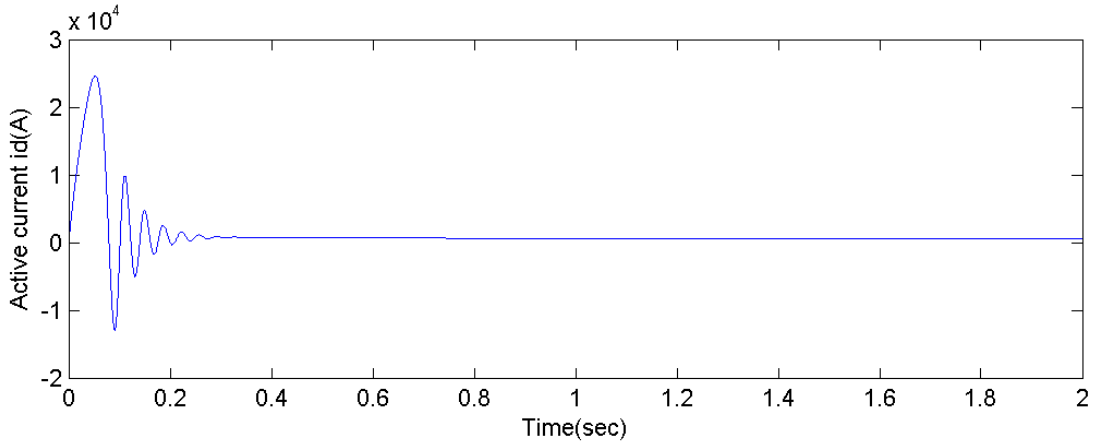

Figure 4.3 i_d response when poles in [-17.21 -17.21 -0.4]

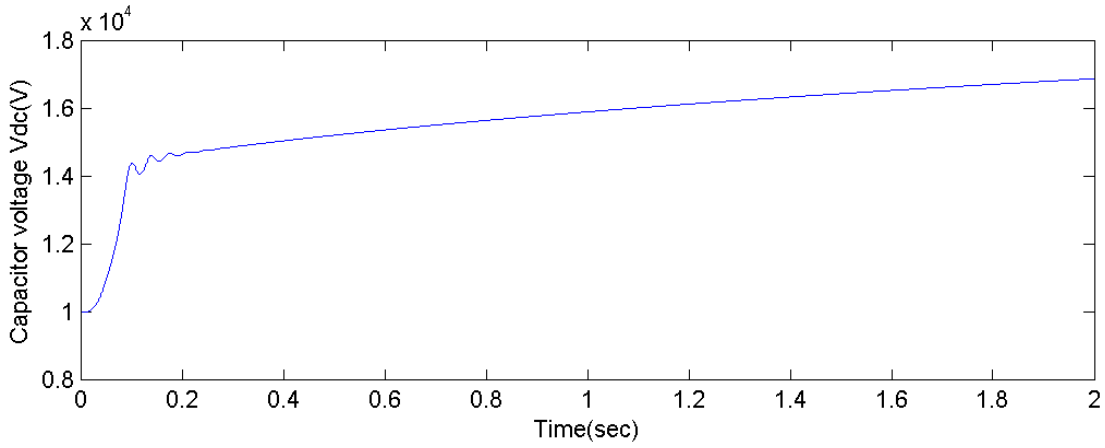

Figure 4.4 V_{dc} response when poles in [-17.21 -17.21 -0.4]

From the above responses it can be concluded that in order to reduce the settling time and to increase damping of the system, the natural frequency of the closed loop system needs to be increased. So in order to achieve that the real part of eigen values for i_q and i_d are further increased by a factor 6.84 and the real part of the eigen value of for pole of V_{dc} is further increased by a factor of ten. So the new values are [-117.12, -117.12, -4]. From the system response shown in Figure 4.5-4.7.we can see that dumping is increased, and there is no oscillation in the system response. However, there is still a large overshoot and steady state error in all three states, and the responses are even worse. One possible reason for this can be that we have changed the relative dynamic characteristics among the i_q, i_d and V_{dc} and they are in fact coupled.

Thus we try to change the relative dynamic characteristics of i_q, i_d and V_{dc} by only increasing the real part of the pole value of V_{dc} by factor ten to before to get the closed loop poles as [-117.12, -117.12, -40]. The system response is shown in Figure 4.8-4.10. We can see that the system response showing that the settling time is reduced to within 0.2 sec in all three states - i_q, i_d and V_{dc}. The voltage of capacitor V_{dc} becomes constant after settling time. It is our desired system dynamic characteristics, except that there are still large overshoot and steady state errors.

We continue to change the system natural frequency by settling the poles far more left in the plane. The real part of the pole values is increased by factor ten to [-1170.12, -1170.12, -400]. From the system response, see Figure 4.11 -4.13, we know that the overshoot for i_d is about 400A and there are no overshoot for i_q and V_{dc}, the steady state error for i_q and i_d are zero while the value for V_{dc} is about 15V. Furthermore, the settling time for all three states deceased to around 0.02sec.

We need to reduce the overshoot of i_d, settling time of all three states, and the steady state error of V_{dc} further such that the requirement are be satisfied. After trial and error we set the poles on [-2570.12, -2570.12, -800]. The system response is shown in Figure 4.14-4.16. The overshoot of i_d reduced to 150V and the settling time for all three states reduced to less than 0.005 sec. Also, the steady state error of capacitor voltage V_{dc} is reduced to less than 2V.

.

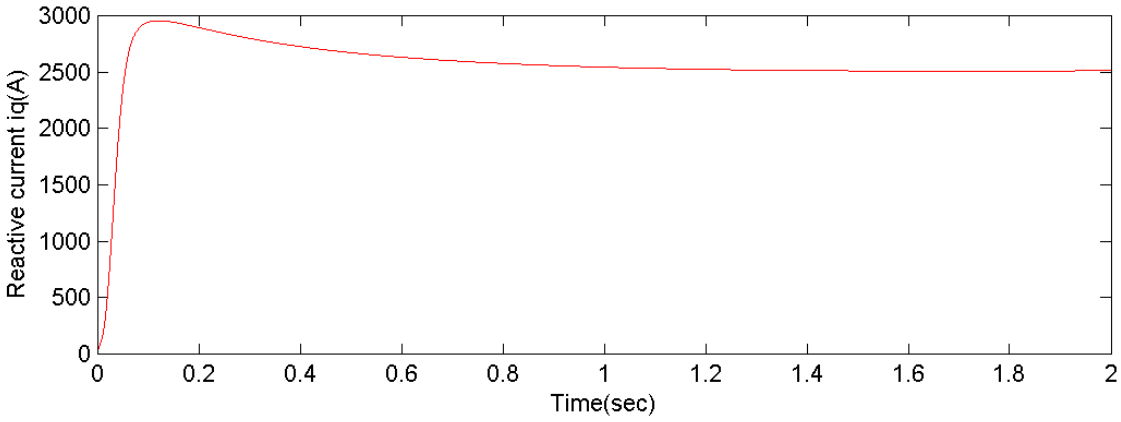

Figure 4.5 i_q response when poles in [-117.21 -117.21 -4]

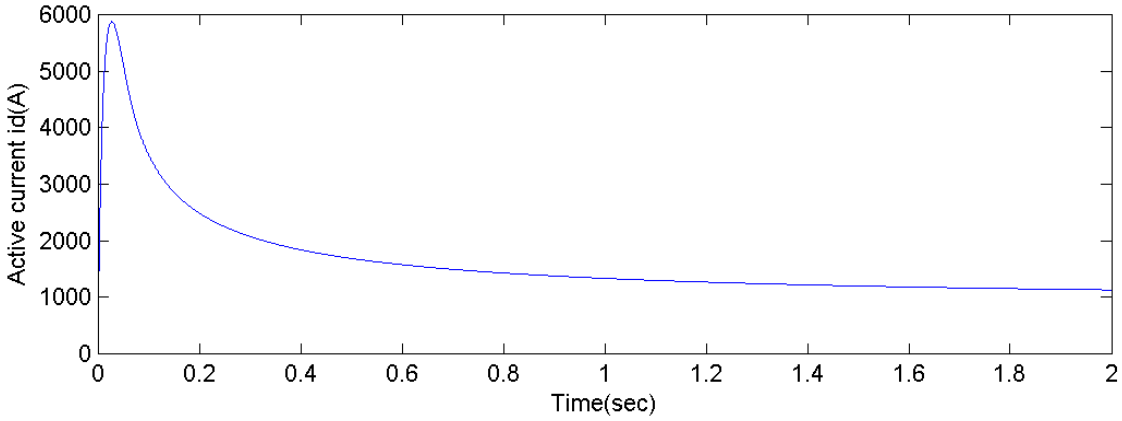

Figure 4.6 i_d response when poles in [-117.21 -117.21 -4]

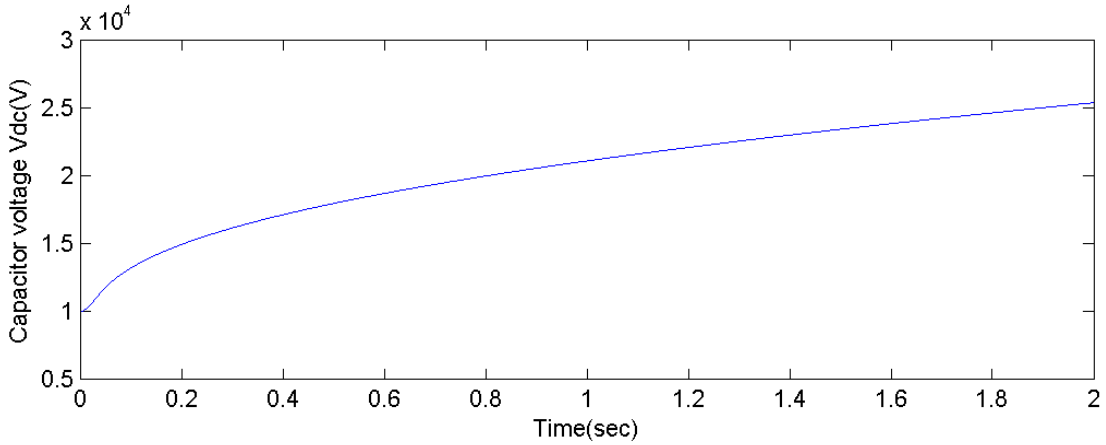

Figure 4.7 V_{dc} response when poles in [-117.21 -117.21 -4]

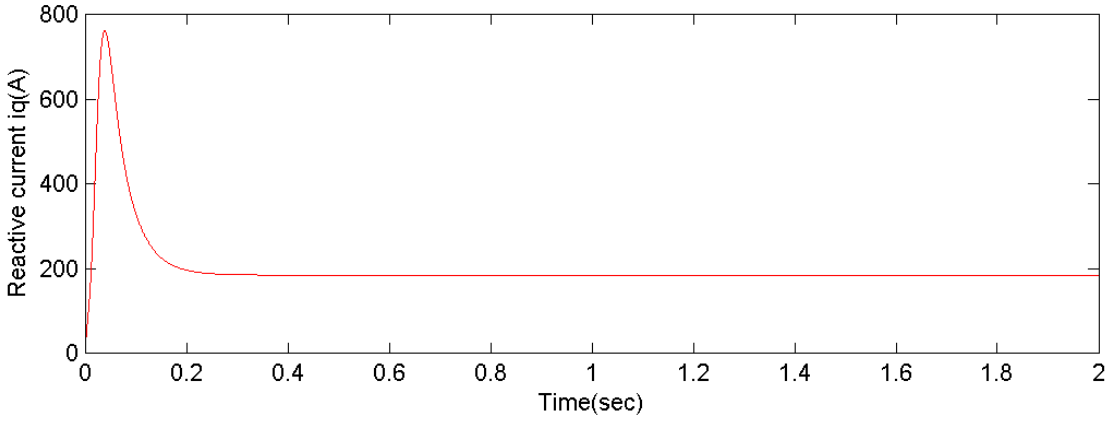

Figure 4.8 i_q response when poles in [-117.21 -117.21 -40]

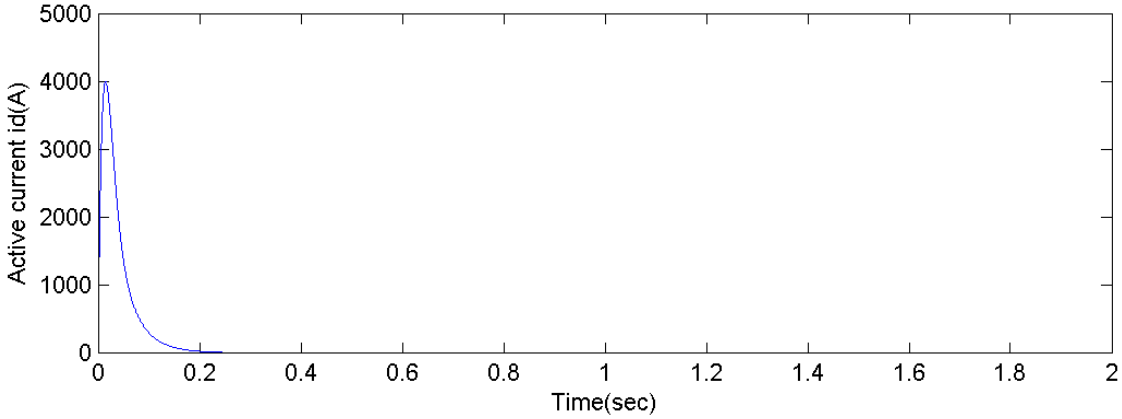

Figure 4.9 i_d response when poles in [-117.21 -117.21 -40]

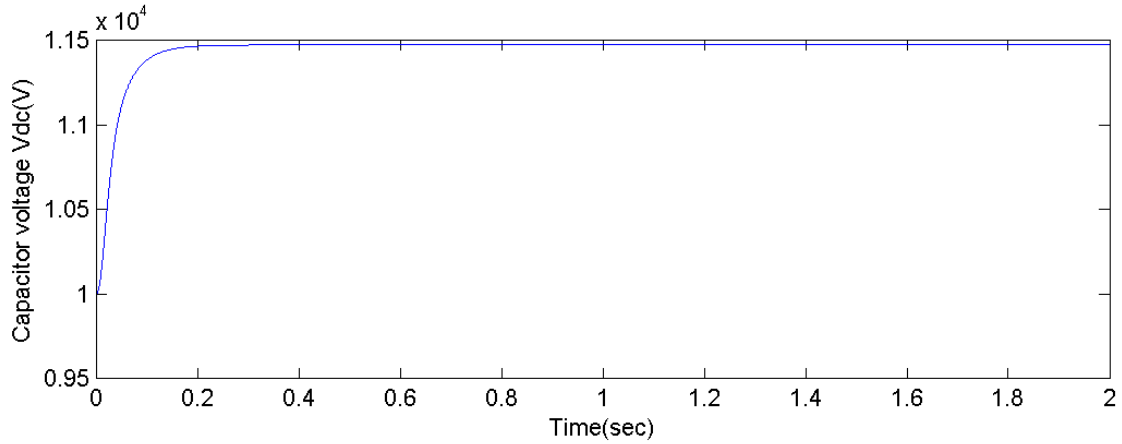

Figure 4.10 V_{dc} response when poles in [-117.21 -117.21 -40]

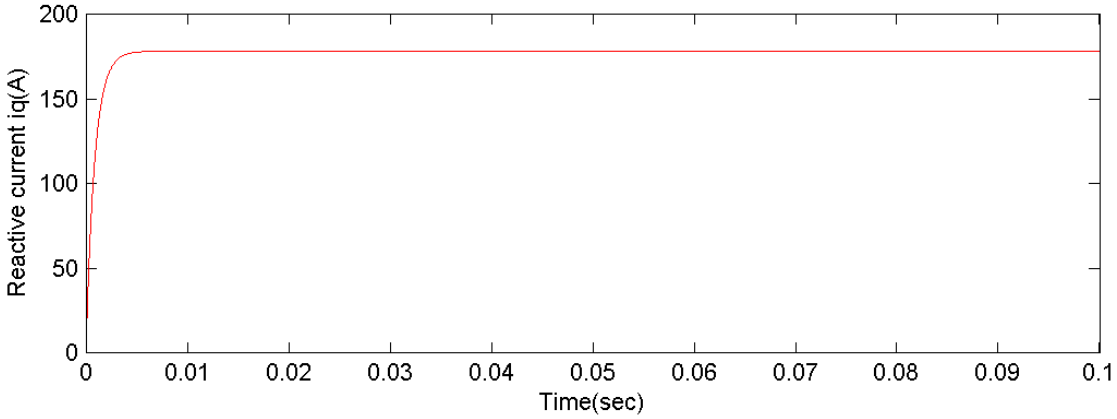

Figure 4.11 i_q response when poles in [-1170.21 -1170.21 -400]

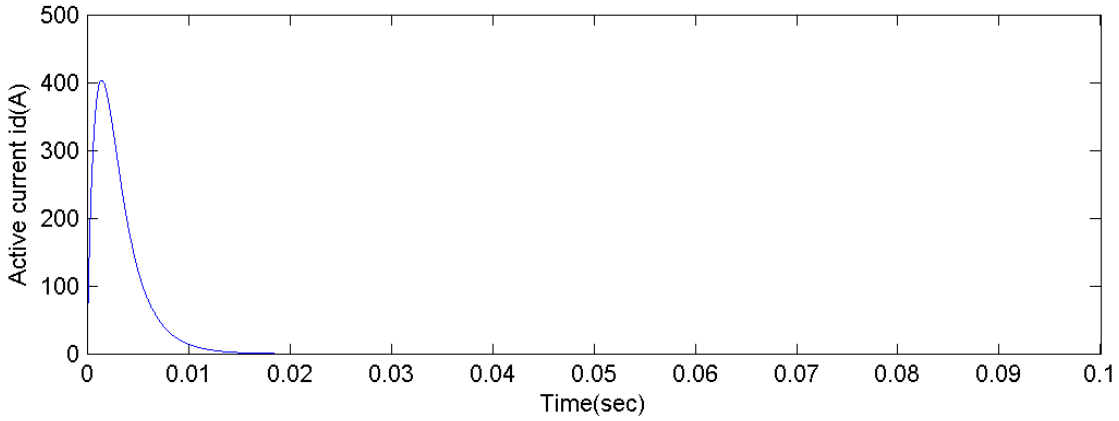

Figure 4.12 i_d response when poles in [-1170.21 -1170.21 -400]

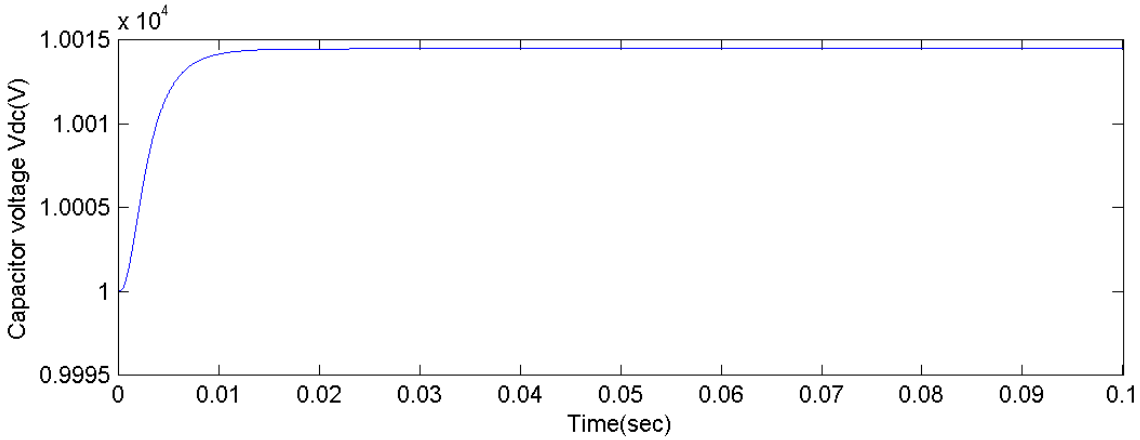

Figure 4.13 V_{dc} response when poles in [-1170.21 -1170.21 -400]

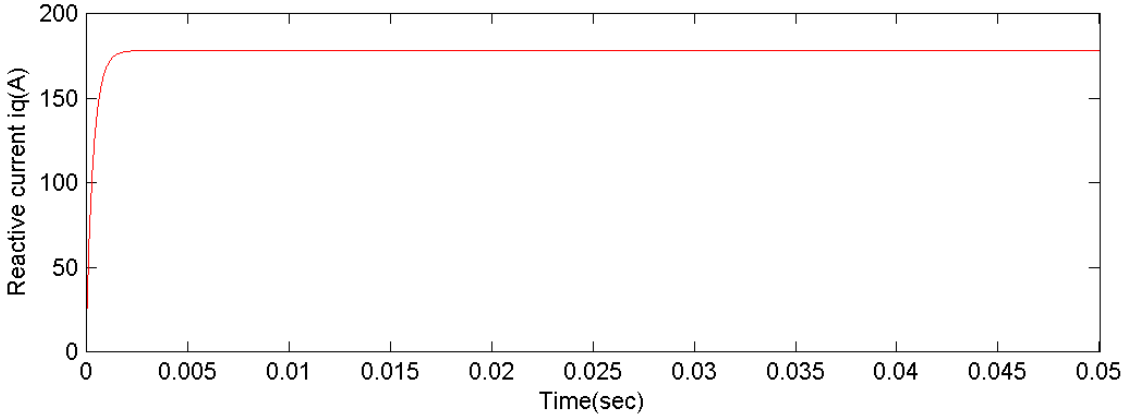

Figure 4.14 i_q response when poles in [-2570.21 -2570.21 -800]

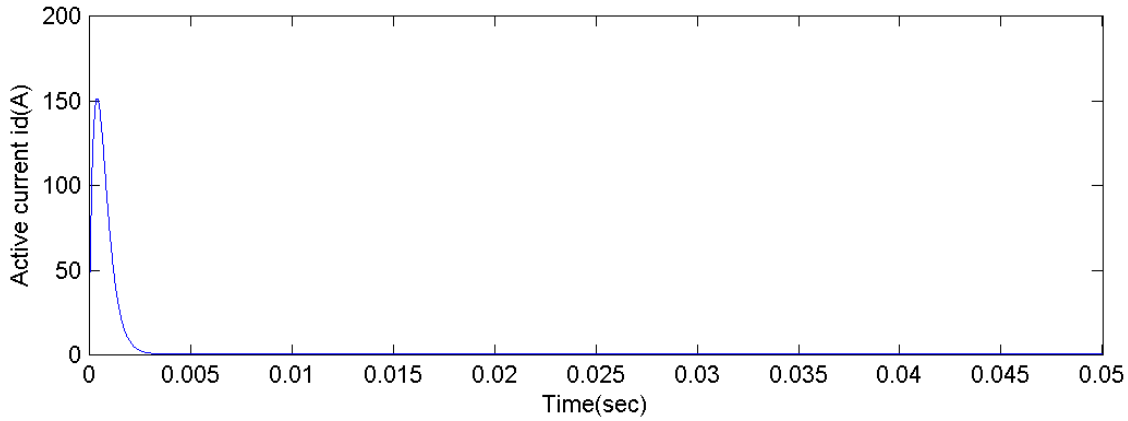

Figure 4.15 i_d response when poles in [-2570.21 -2570.21 -800]

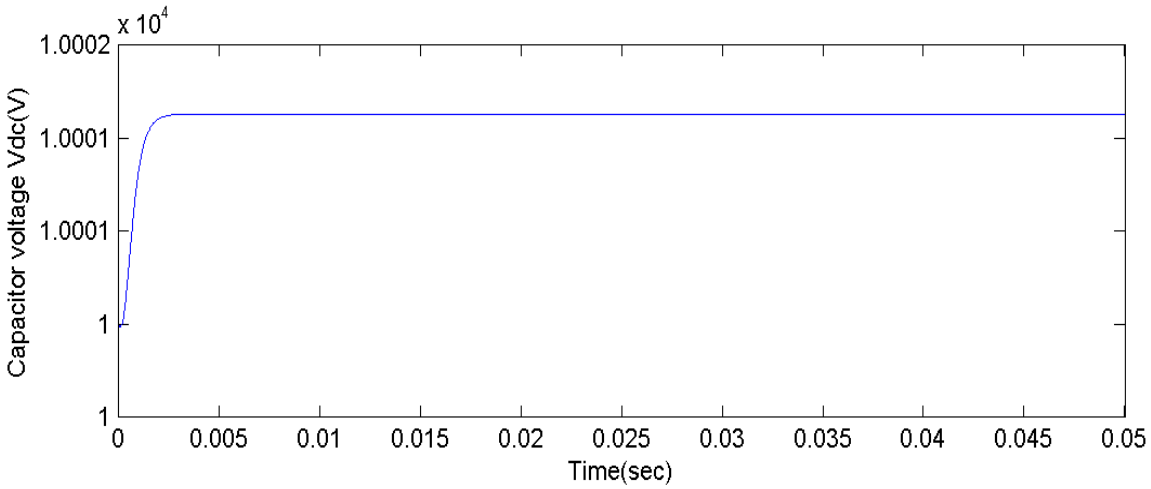

Figure 4.16 V_{dc} response when poles in [-2570.21 -2570.21 -800]

We also need to consider is the control effort limitation of Dd and Dq, which should be within [-1, +1]. Figure 4.17 shows the control effort of Dq and Dd in the last situation when poles being assigned to [-2570.12, -2570.12, -800]. From this Figure we know that the Dd and Dq satisfy the hardware requirement.

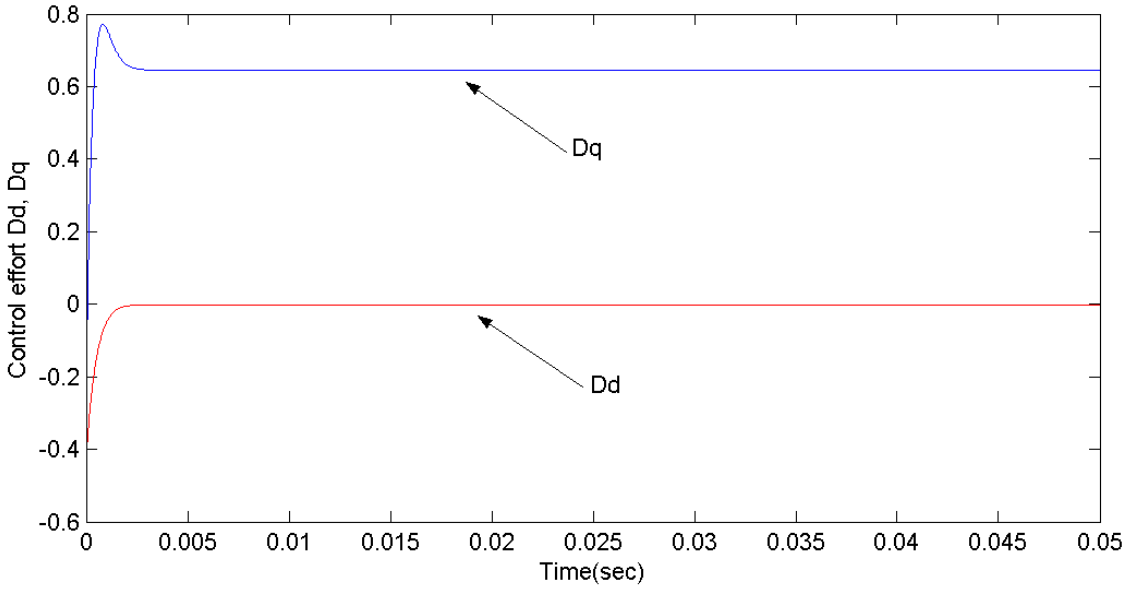

Figure 4.17 Control effort Dd and Dq when pole in[-2501.12, -2570.12, -800]

4.2 LQR Controller Design

Another MIMO design approach is the optimal control method linear quadratic regulator (LQR). The idea is to transfer the designer's iteration on pole locations as used in full state feedback to iterations on the elements in a cost function, J. This method determines the feedback gain matrix that minimizes J in order to achieve some compromise between the use of control effort, the magnitude, and the speed of response that will guarantee a stable system.

4.2.1 Algorithm

For a given system:

$$\dot{x} = Ax + Bu; \tag{4.6}$$

determine the matrix K of the LQR vector

$$u(t) = -Kx(t) \tag{4.7}$$

so in order to minimize the performance index,

$$J = \int_0^\infty (x^T Q x + u^T R u) dt \qquad (4.8)$$

where Q and R are the positive-definite Hermitian or real symmetric matrix. Note that the second term on the right side account for the expenditure of the energy on the control efforts. The matrix Q and R determine the relative importance of the error and the expenditure of this energy.

From the above equations we get

$$J = \int_0^\infty (x^T Q x + x^T K^T R K x) dt = \int_0^\infty x^T (Q + K^T R K) x dt \qquad (4.9)$$

following the discussion given in solving the parameter-optimization problem, we set

$$x^T (Q + K^T R K) x = -\frac{d}{dt}(x^T P x) \qquad (4.10)$$

then we obtain

$$x^T (Q + K^T R K) x = -\dot{x}^T P x - x^T P \dot{x} = -x^T [(A - BK)^T P + P(A - BK)] x \qquad (4.11)$$

comparing both sides of the above equation and note that this equation must hold true for any x, we require that

$$(A - BK)^T P + P(A - BK) = -(Q + K^T R K). \qquad (4.12)$$

Since R has been assumed to be a positive-definite Hermitian or real symmetric matrix, we can write

$$R = T^T T$$

where T is a nonsingular matrix.

and

$$A^T P + PA + [TK - (T^T)^{-1} B^T P]^T [TK - (T^T)^{-1} B^T P] - PBR^{-1} B^T P + Q = 0. \qquad (4.13)$$

The minimization of J with respect to K requires the minimization of

$$x^T [TK - (T^T)^{-1} B^T P]^T [TK - (T^T)^{-1} B^T P] x. \qquad (4.14)$$

Which this equation is nonnegative, the minimum occurs when it is zero, or when

$$TK = (T^T)^{-1} B^T P. \qquad (4.15)$$

Hence

$$K = T^{-1} (T^T)^{-1} B^T P = R^{-1} B^T P. \qquad (4.16)$$

Thus we get a control law as

$$u(t) = -Kx(t) = -R^{-1}B^{T}Px(t) \qquad (4.17)$$

in which P must satisfy the reduced Riccati equation:

$$A^{T}P + PA - PBR^{-1}B^{T}P + Q = 0 \qquad (4.18)$$

4.2.2 Weight Matrix Selection

The LQR design selects the weight matrix Q and R such that the performances of the closed loop system can satisfy the desired requirements mentioned earlier.

The selection of Q and R is weakly connected to the performance specifications, and a certain amount of trial and error is required with an interactive computer simulation before a satisfactory design results.

4.2.3 Controller Design

Since the matrix Q and R are symmetric so there are 6 distinct elements in Q and 3 distinct elements in R for a total of 9 distinct elements need to be selected. And also the matrix Q and R should satisfy the positive definitions. One practical method is to set Q and R to be diagonal matrix such that only five elements need to be decided. The value of the elements in Q and R is related to its contribution to the cost function J.

In our case, the response requirement of i_q and i_d are the same, but the response requirement of V_{dc} is slow. Thus we first select the diagonal elements of Q and R as *diag* [Q]= [0.05, 0.05, 0.005] and *diag* [R]= [1, 1]. The system response is shown in Figure 4.18-4.20. We can find that the response of i_q is perfect but the i_d and V_{dc} do not converge within 2 sec.

We need pay more cost weight to V_{dc} in order to satisfy the requirement. We set diagonal elements of Q and R to *diag* [Q]= [0.05, 0.05, 0.01] and *diag* [R]= [1, 1]. The system response is shown in Figure 4.21-4.23. The response of V_{dc} and i_d converge to the desired constant value this time, but the settling time is about 0.6sec, which is much higher than the requirement (less than 0.017 sec).

Next we increase cost of V_{dc}, set the diagonal elements of Q and R to *diag* [Q]=[0.05, 0.05, 100] and *diag* [R]= [1, 1]. From Figure 4.24-4.26 we can see that the settling time of V_{dc} and i_d are within 0.015sec, which means they satisfy the design requirements. And the steady state errors of i_q, i_d and V_{dc} also satisfy the requirements. But when we check the control effort, shown in Figure 4.27, we can see that the maximum value of the control effort of *Dd* is about -13, which is much bigger than the hardware limitation value [-1, +1], which means we need to adjust matrix R.

Thus we need to increase the cost weight of *Dd* by changing matrix R's the diagonal elements to *diag* [R] = [45, 400]. The system response is shown in Figure 4.28-31. In this case we find that all the three states dynamic responses satisfied the requirements. Also, the mean time of the control effort *Dd* and *Dq* are within the limitation.

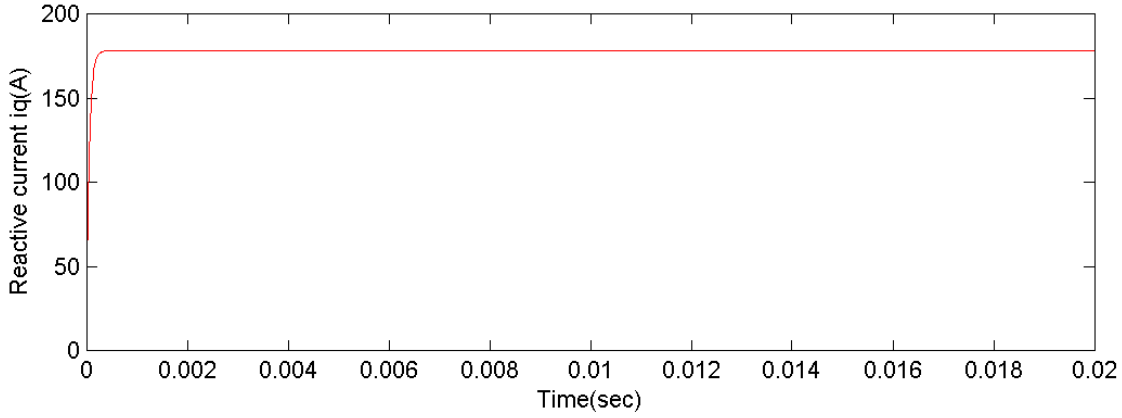

Figure 4.18 i_q response when *diag* [Q]= [0.05, 0.05, 0.005] and *diag* [R]= [1, 1].

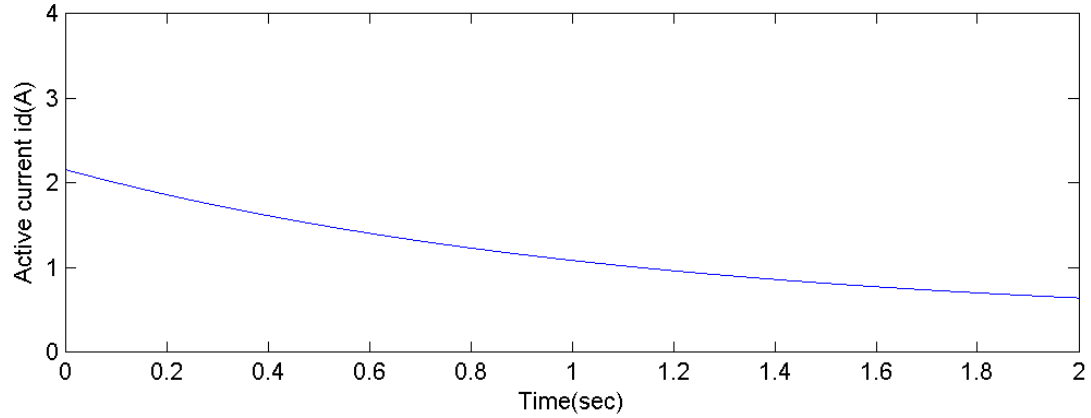

Figure 4.19 i_d response when *diag* [Q]= [0.05, 0.05, 0.005] and *diag* [R]= [1, 1].

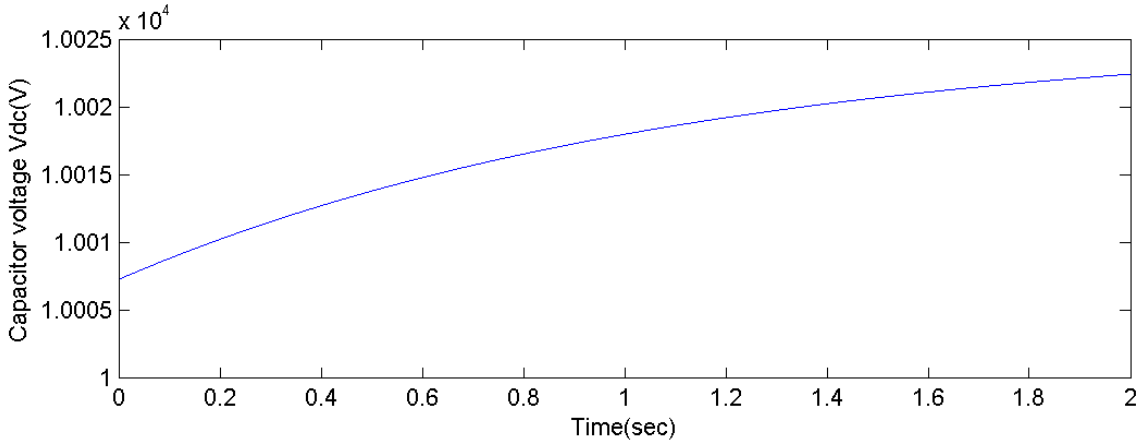

Figure 4.20 *Vdc* response when *diag* [Q]= [0.05, 0.05, 0.005] and *diag* [R]= [1, 1].

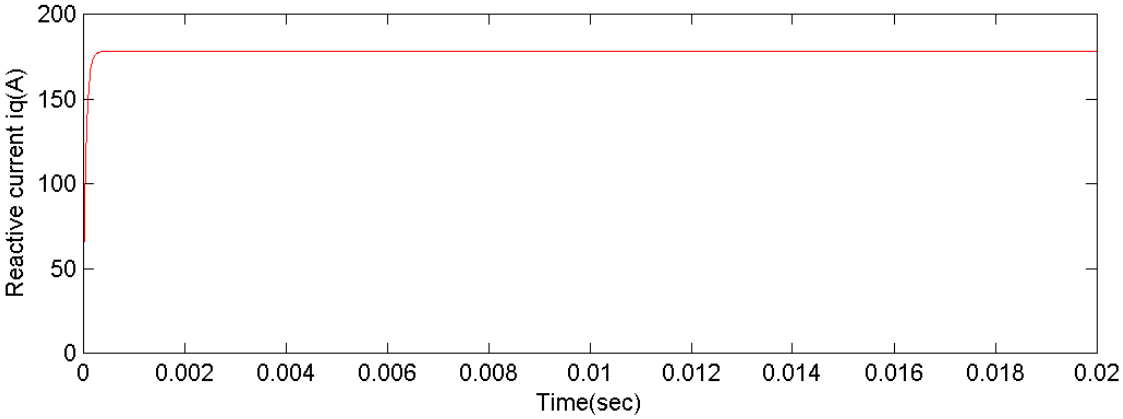

Figure 4.21 i_q response when *diag* [Q]= [0.05, 0.05, 0.01] and *diag* [R]= [1, 1].

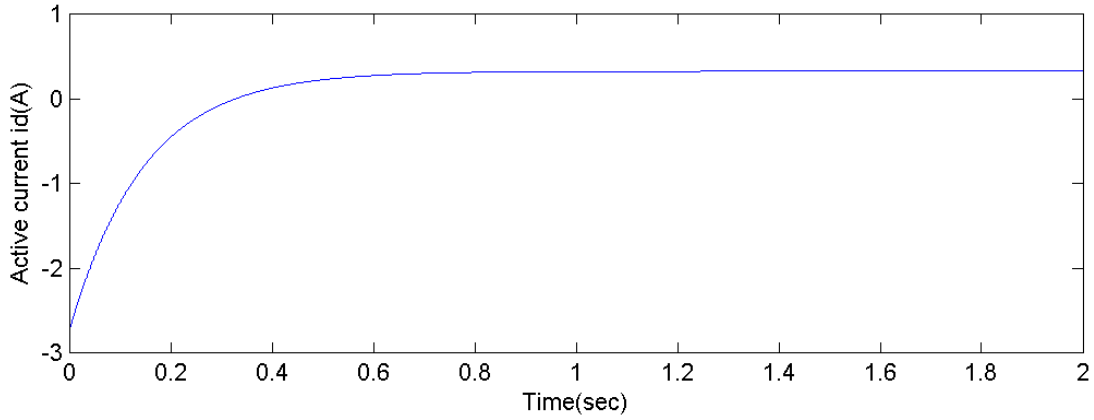

Figure 4.22 i_d response when *diag* [Q]= [0.05, 0.05, 0.01] and *diag* [R]= [1, 1].

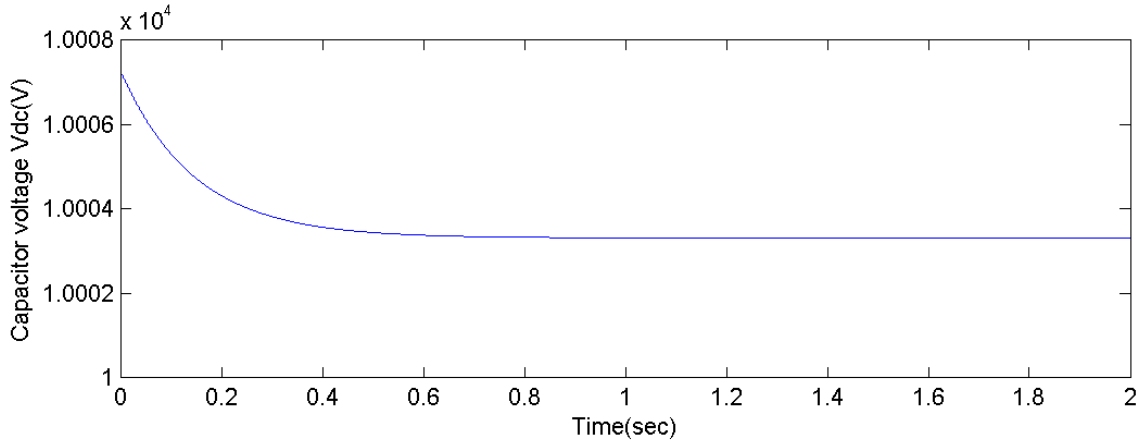

Figure 4.23 *Vdc* response when *diag* [Q]= [0.05, 0.05, 0.01] and *diag* [R]= [1, 1].

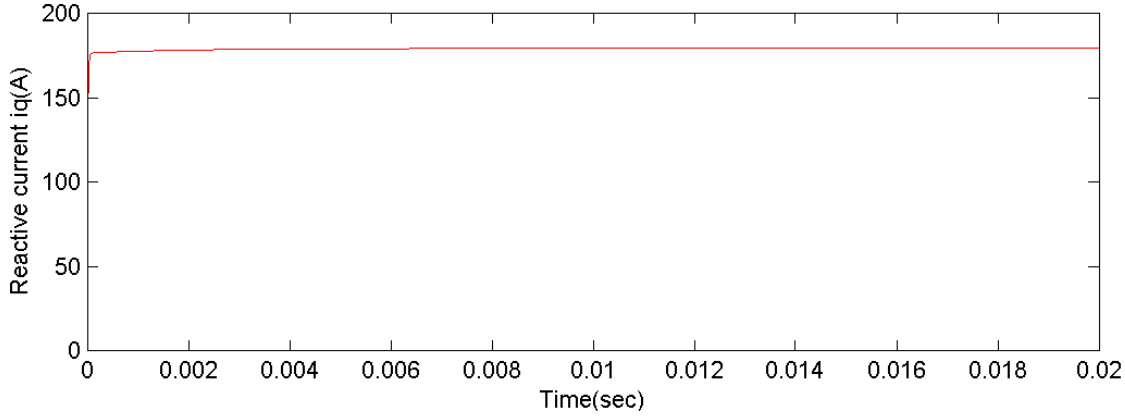

Figure 4.24 i_q response when *diag* [Q]=[0.05, 0.05, 100] and *diag* [R]= [1, 1].

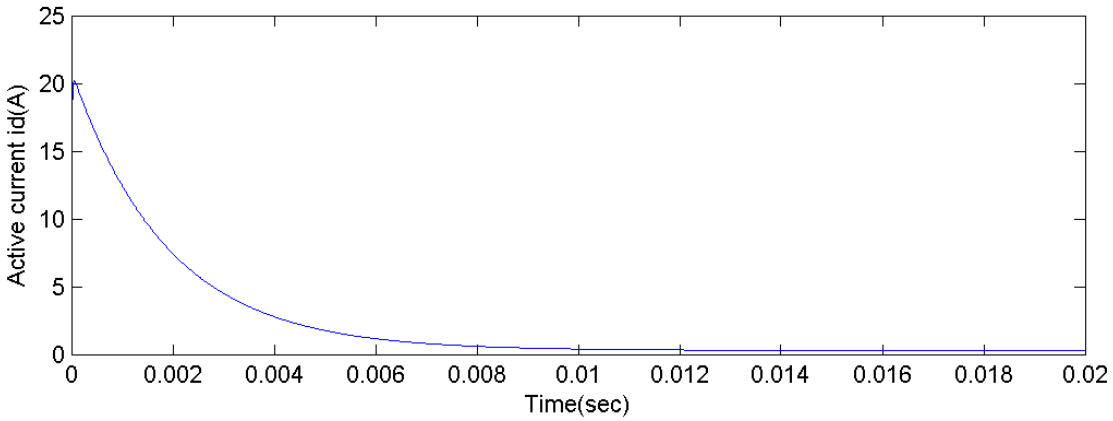

Figure 4.25 i_d response when *diag* [Q]=[0.05, 0.05, 100] and *diag* [R]= [1, 1].

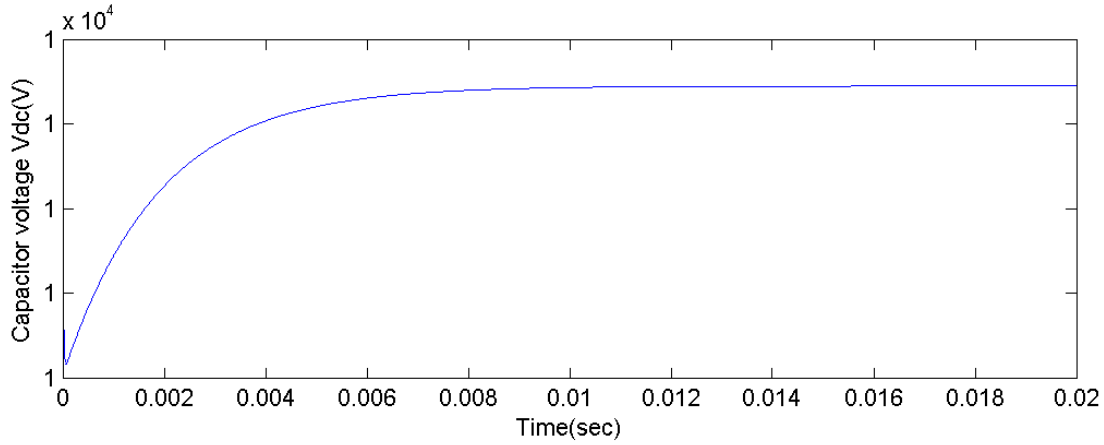

Figure 4.26 *Vdc* response when *diag* [Q]=[0.05, 0.05, 100] and *diag* [R]= [1, 1].

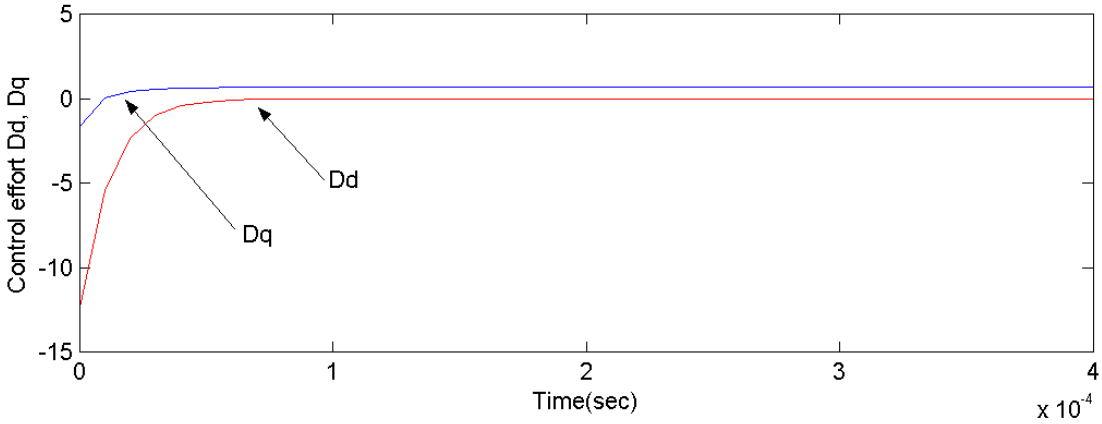

Figure 4.27 *Dd* and *Dq* when *diag* [Q]=[0.05, 0.05, 100] and *diag* [R]= [1, 1].

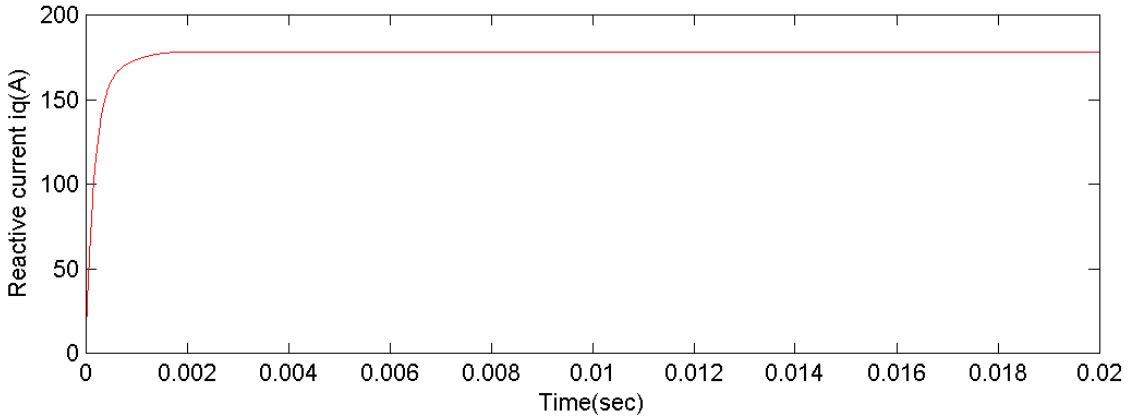

Figure 4.28 i_q response when *diag* [Q]=[0.05, 0.05, 100] and *diag* [R] = [45, 400].

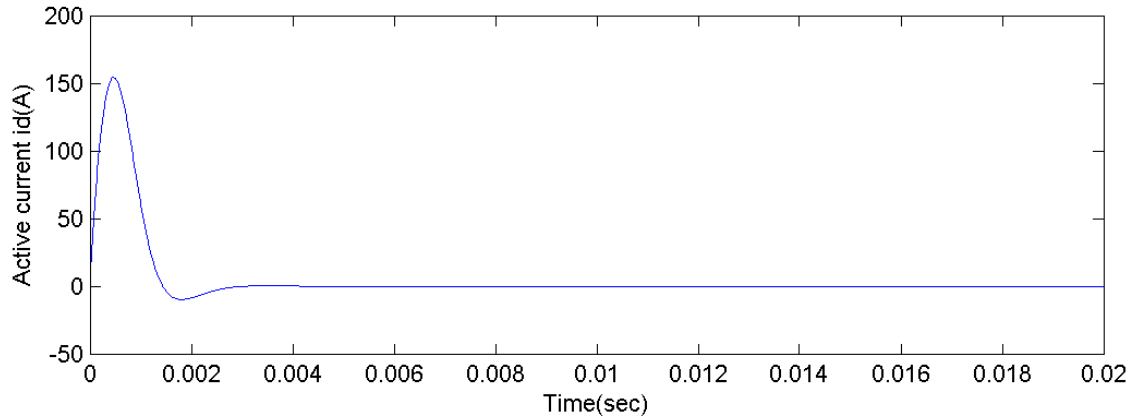

Figure 4.29 i_d response when *diag* [Q]=[0.05, 0.05, 100] and *diag* [R] = [45, 400].

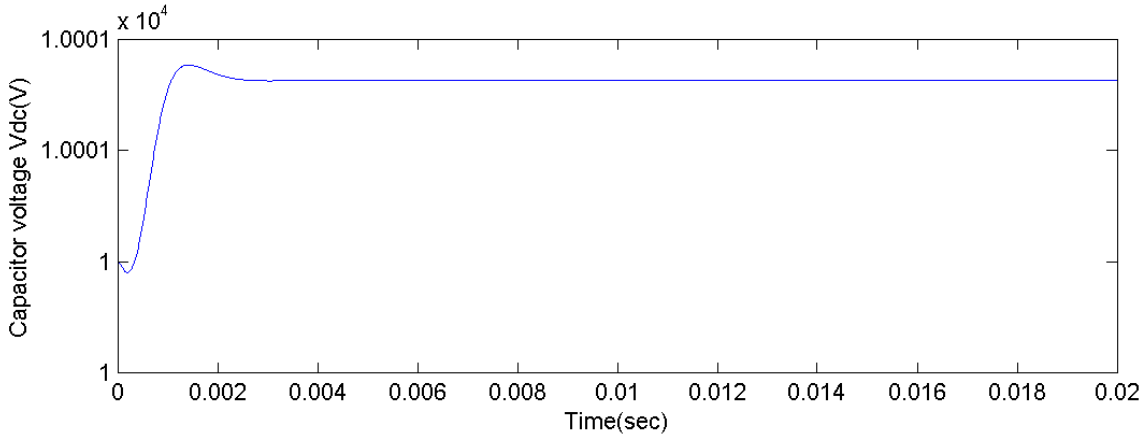

Figure 4.30 V_{dc} response when *diag* [Q]=[0.05, 0.05, 100] *diag* [R] = [45, 400].

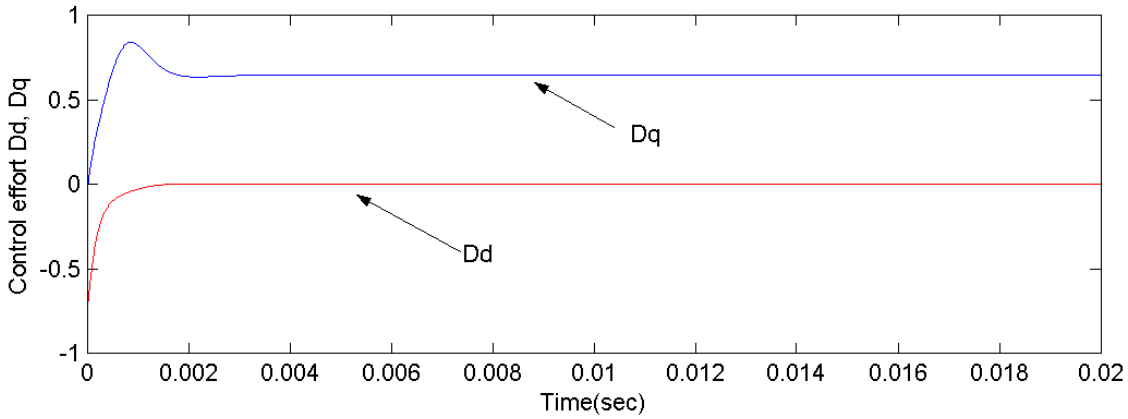

Figure 4.31 *Dd* and *Dq* when *diag* [Q]=[0.05, 0.05, 100] and *diag* [R] = [45, 400].

4.3. Comparison of Different Design Methods

From previous discussion we know that both of pole assignment and LQR approach can be used to design the controller of STATCOM. However, we need do some performance comparisons between these two methods to find out which one is more suitable for our application.

4.3.1 Controller Performance

The main purpose of the STATCOM is to output the reference i_q* which depend on the connected power system condition. Thus we can look the control loop as a state feedback loop with reference input vector X*. That means the control loop should make i_q track the value of i_q* as quick as possible meanwhile keeping V_{dc} and i_d as desired constant. The symbol "*" is used to indicate the reference value.

Although these two control methods show us almost the same good performance on the operating point, it is necessary to investigate their robustness. So we need to see the system performance when i_q* change from its operating point (178A).

First we make the i_q* as a step change from 178A to 267A (increase 50%). Figure 4.32 show the system response by using pole assignment method. Figure 4.33 show the system response by using LQR method. In each loop we set i_q* have step change from 178A to 267A at the time of 0.015sec. Both of them show their good robust characteristics to the change of i_q*.

Then we make the i_q* as a step change from 267A (increase 50% from 178A) to 89A (decrease 50% from 178A). Figure 4.34 show the system response by using pole assignment method. Figure 4.35 show the system response by using LQR method. In each loop we set i_q* have step change from 267A (+50%) to 89A (-50%) at the time of 0.015sec. Again, both of them show their good robust characteristics to the change of i_q*.

4.3.2 Pole Assignment –LQR Design Procedure Comparison

1. Pole assignment method

Pole location must be chosen carefully and wisely, which needs deep insight of the system characteristics. Also, for the multi-input multi-output system as in this case, the gain matrix K is not uniquely determined by the resulting equations. Thus it is not easy to use pole assignment method to design a MIMO system. We need higher feedback gain to reduce the system response time and attenuate disturbances that might enter the system. But higher gain leads to higher input that is limited by the hardware.

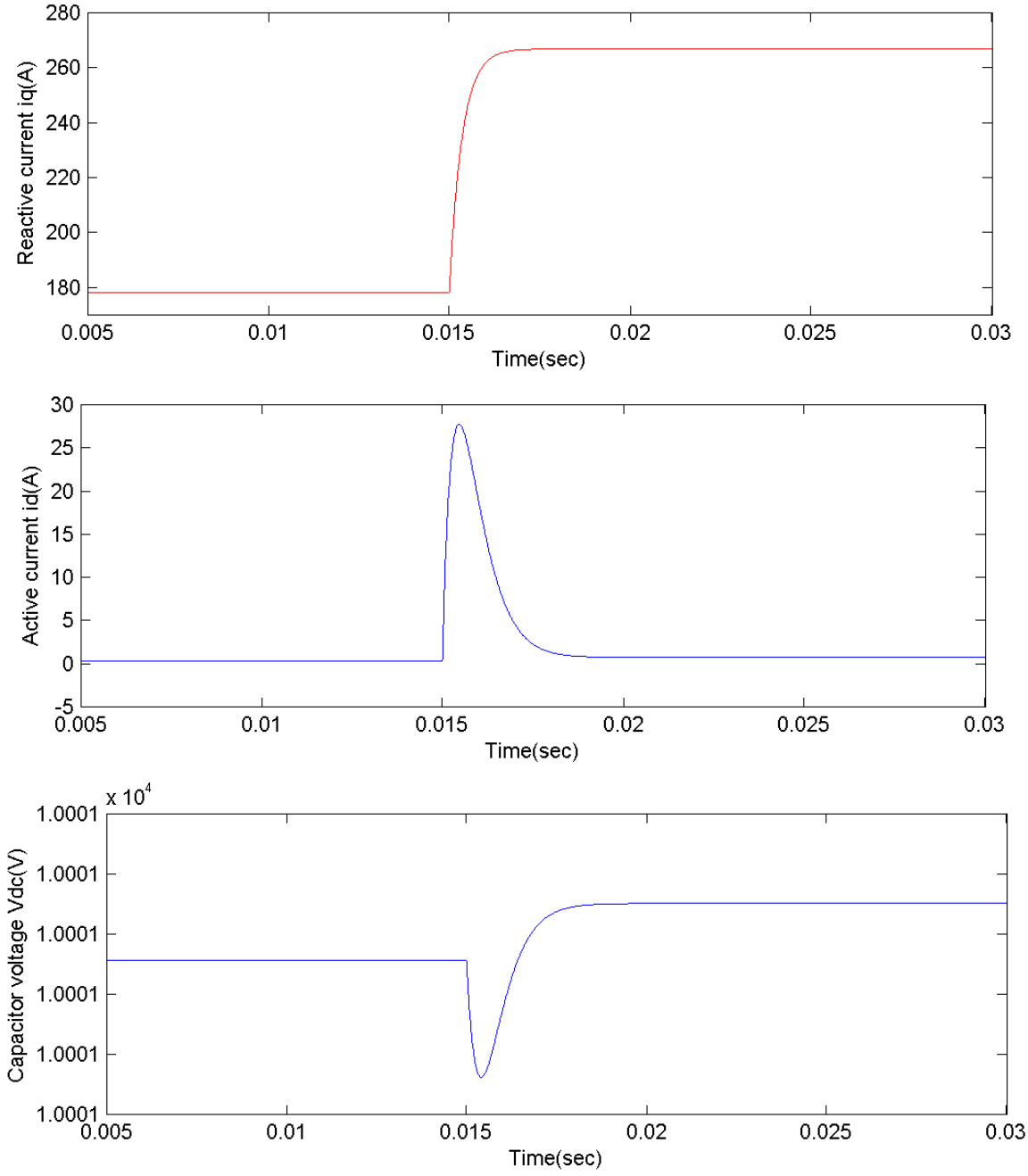

Figure 4.32 System response to a change in the reference reactive current i_q* from 178A to 267A by using pole assignment controller

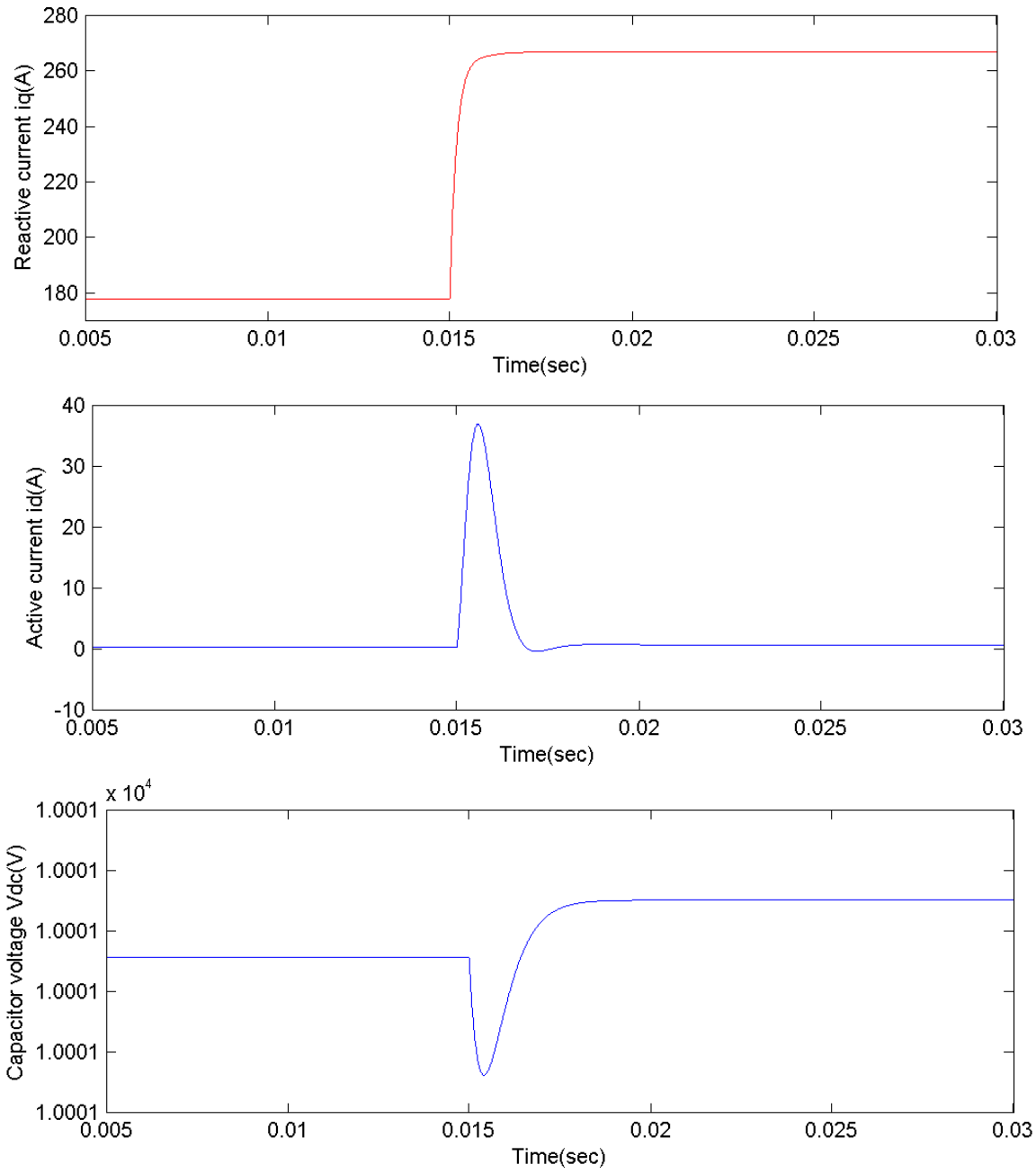

Figure 4.33 System response to a change in the reference reactive current i_q* from 178A to 267A by using LQR controller

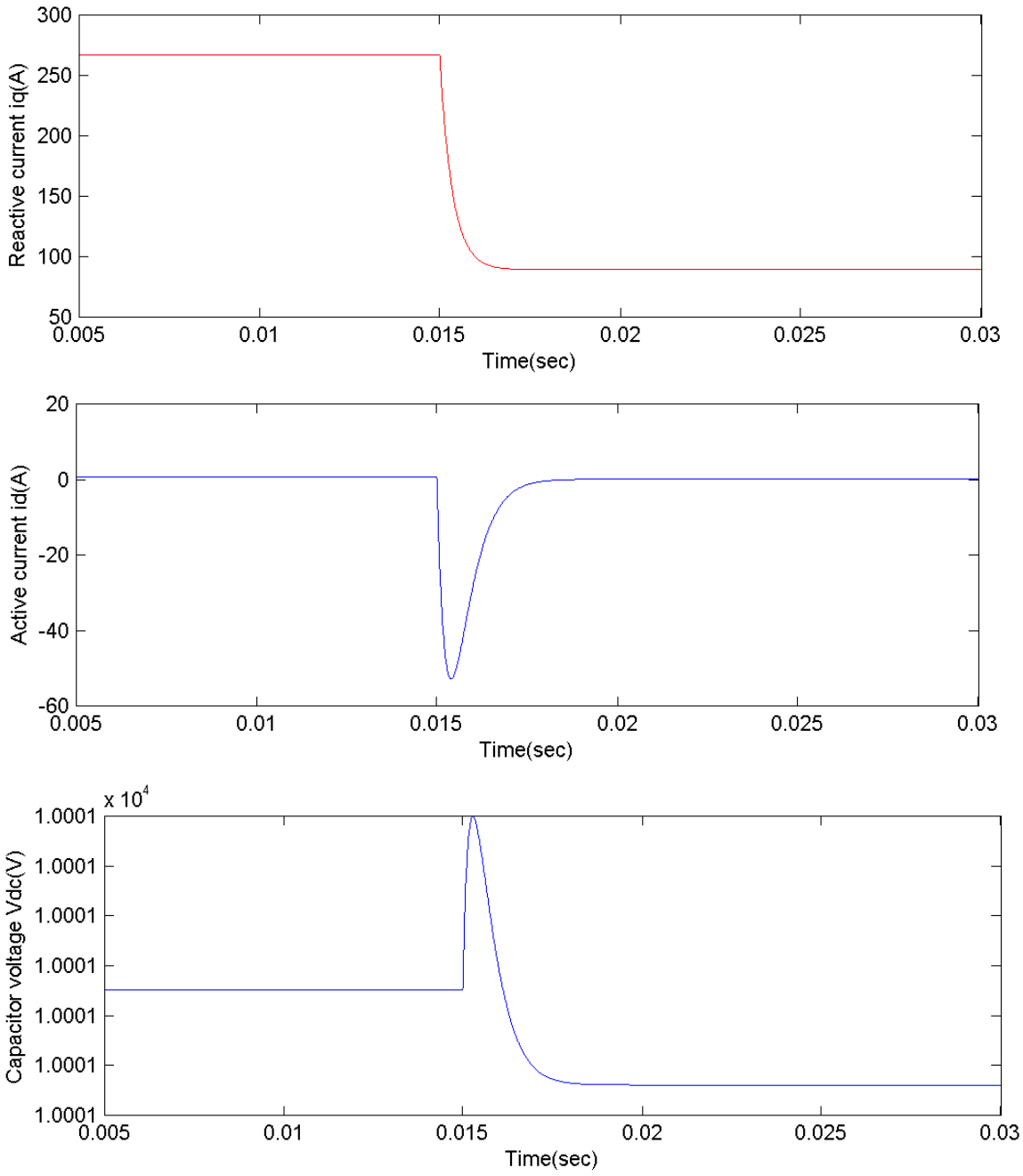

Figure 4.34 System response to a change in the reference reactive current i_q* from 267A to 89A by using pole assignment controller

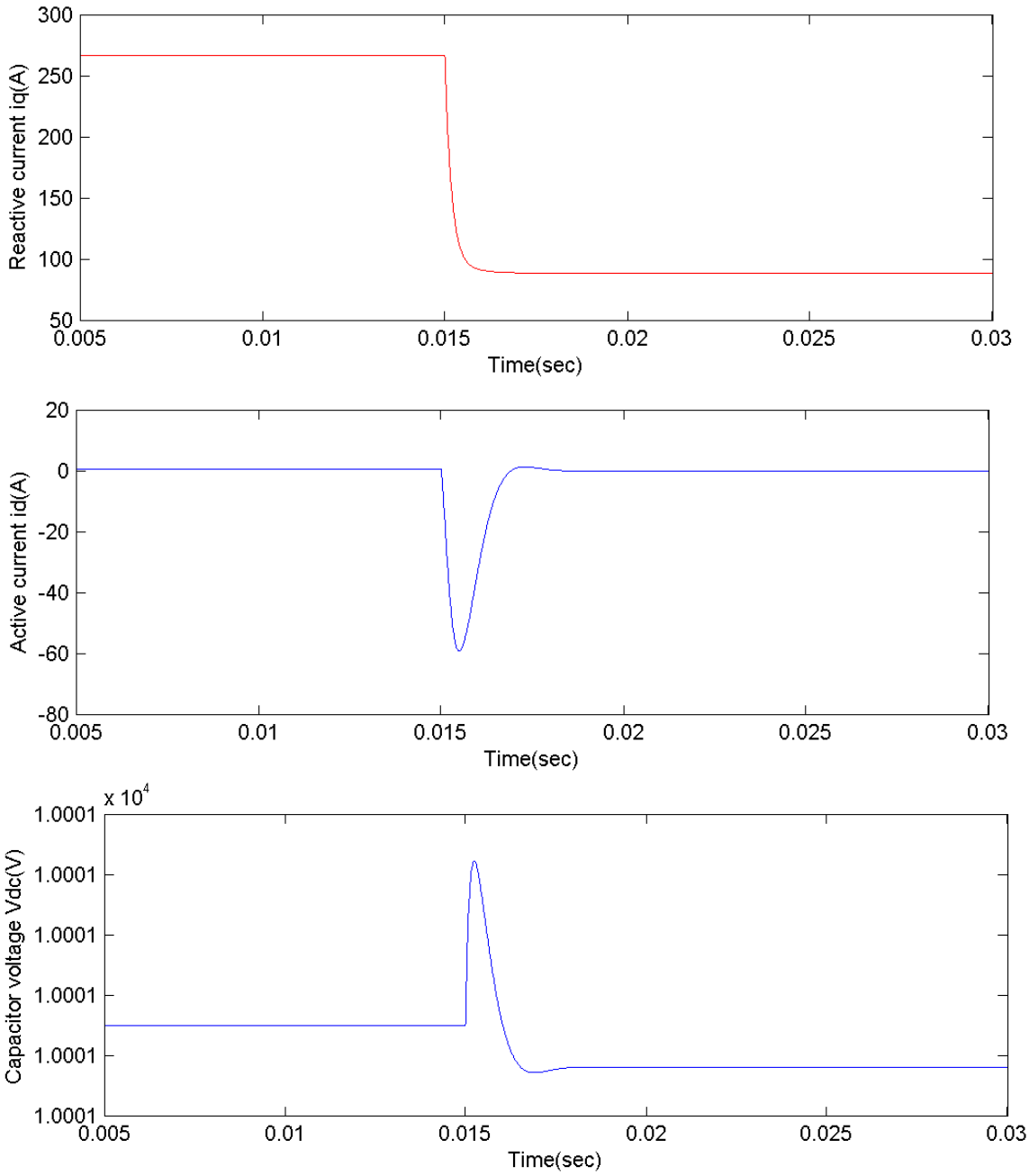

Figure 4.35 System response to a change in the reference reactive current i_q* from 267A to 89A by using LQR controller

4.3.3 Pole Assignment –LQR Design Procedure Comparison

2. Pole assignment method

Pole location must be chosen carefully and wisely, which needs deep insight of the system characteristics. Also, for the multi-input multi-output system as in this case, the gain matrix K is not uniquely determined by the resulting equations. Thus it is not easy to use pole assignment method to design a MIMO system. We need higher feedback gain to reduce the system response time and attenuate disturbances that might enter the system. But higher gain leads to higher input that is limited by the hardware.

Thus we need to make a compromise between the input energy and output performance and pay lots of attention while selecting the poles. It is still hard to find a solution that can satisfy all the requirements.

3. LQR method

By using LQR, we can use all the freedom of MIMO system and achieve some compromise between the use of control effort and system performance, and can also guarantee a stable system.

We still need to specify the parameters (Q and R) of the cost function J based on the physical specifications. But it is relatively easy to achieve all the requirements. The minimum value of J leads to an unique solution of K, gain matrix.

The quadratic cost function provides us with performance trade-offs among various performance criteria. The relationship between cost function weights and the performance criteria hold for high order and multiple-input system like STATCOM. Therefore it enables the systematic design for multivariable systems.

The selection of Q and R also need a certain amount of trial and error before a satisfactory design results.

4. When sensor noise or system disturbance exist

Both of the two design procedures, pole assignment and LQR, make the assumption that there is no sensor noise or system disturbance inputs to the closed loop systems. This is a fairly restrictive problem statement, since real world control systems are subject to noise and disturbance inputs, especially STATCOM. The circuit of

STATCOM is a switching circuit rather than a continuous circuit. There are significant higher order harmonics that exist in the system. So, in the future work we need to consider these disturbances in real implementations. There is no way to do this for pole assignment design approach. But if we can classify the type of disturbances, we can minimize their effect during the controller design procedure by using stochastic optimal methods such as linear quadratic gaussian method LQG [22].

CHAPTER 5

CIRCUIT VALIDATION WITH BOTH CONTROL METHODS

The proposed control is designed analytically and then tested by circuit simulation to verify the performance of STATCOM. Figure 5.1 shows the experimental diagram set up in the computer aided design, schematic capture, and simulation package POWERSIM. The controller block represents the pole assignment method shown in (4.1)-(4.5). *T* and *T*' blocks represent the vector transformation of power system parameters shown in (2.12). The nonlinear load causes the reactive power change in system by affecting change in the power factor of the load. By using STATCOM, this change can be compensated within one period (0.017sec), as discussed earlier in chapter 4.

In the test, we set the nonlinear load switch into the power system at the time point of 0.5sec. The nonlinear load provides a change in power factor which results in a 25% reduction in i_q*, the reactive current reference, from 178A to 134A. Figure 5.2-4 show i_q, i_d and V_{dc} waveforms of the test power system. The ripples in the waveform i_q and i_d are caused by switching devices in the circuit, these are characteristics of power electronics. From the power system point of view, one typically cares about the average values. So we only analyze the average value in the waveforms.

The i_q changes from 178A to 134A. Meanwhile i_d and V_{dc} keep their steady state values around 0A and 10000V± 1% respectively. Figure 5.5-7 shows zoom-in pictures of

these waveforms. From the waveforms we can see that the i_q can track the change within 0.006sec. The transient response of i_d and V_{dc} are similarly fast.

The test results show that the STATCOM can compensate the reactive power effectively and the control for STATCOM is good enough to ensure the fast reactive power compensation.

Figure 5.8-13 show the results on the same situation by using LQR controller. We found that the results are relatively identical to those by using pole assignment. Even though the gains determined vary by as much as 12%.

Considerable effort in this controller design at this point came from Dr. Li, Electrical and Computer Engineering Department of Florida State University. Dr. Li contributed simulation and modeling support that directly impacted simulation results shown in Fig.5.1 to Fig.5.13.

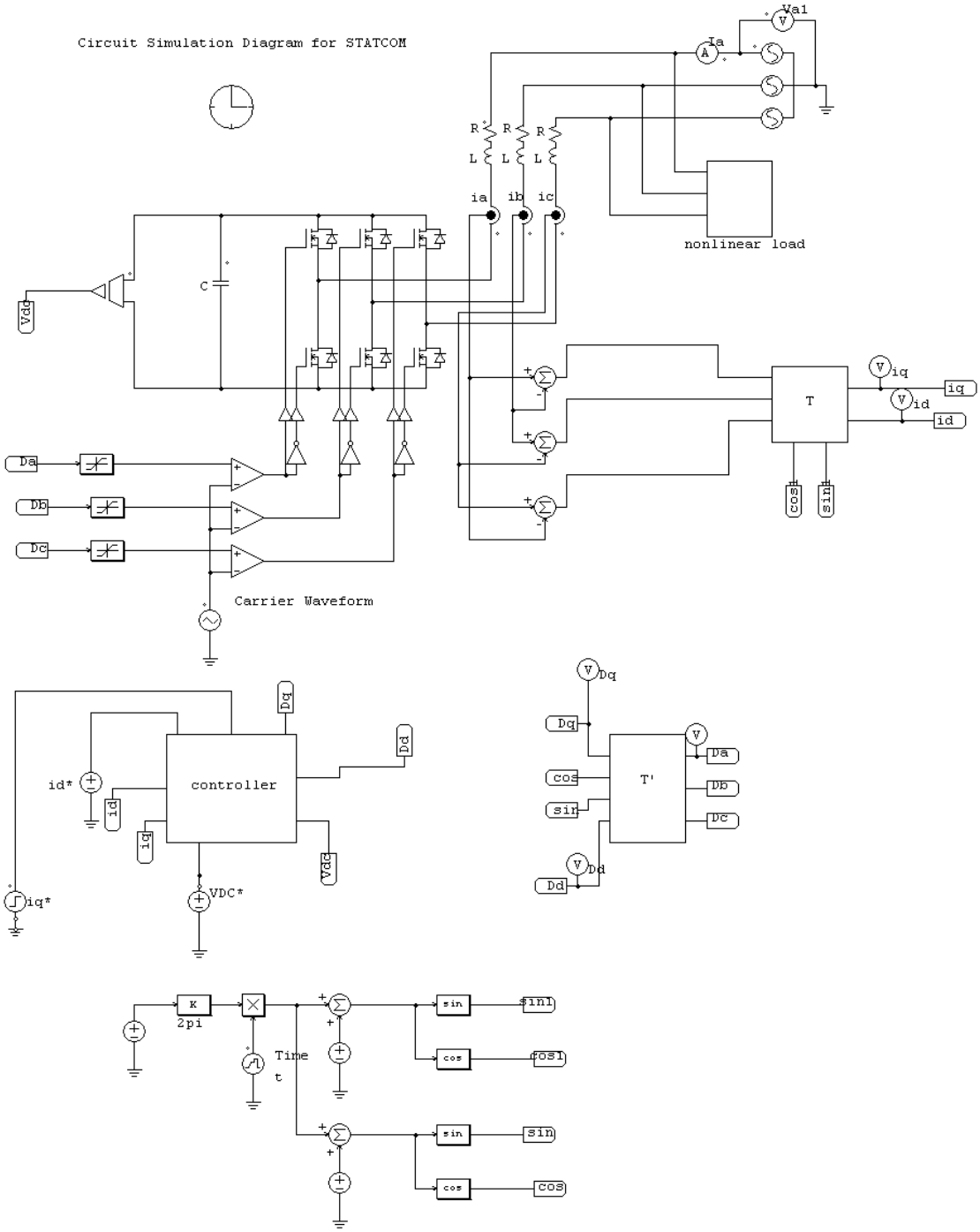

Figure 5.1 Circuit simulation diagram for STATCOM control

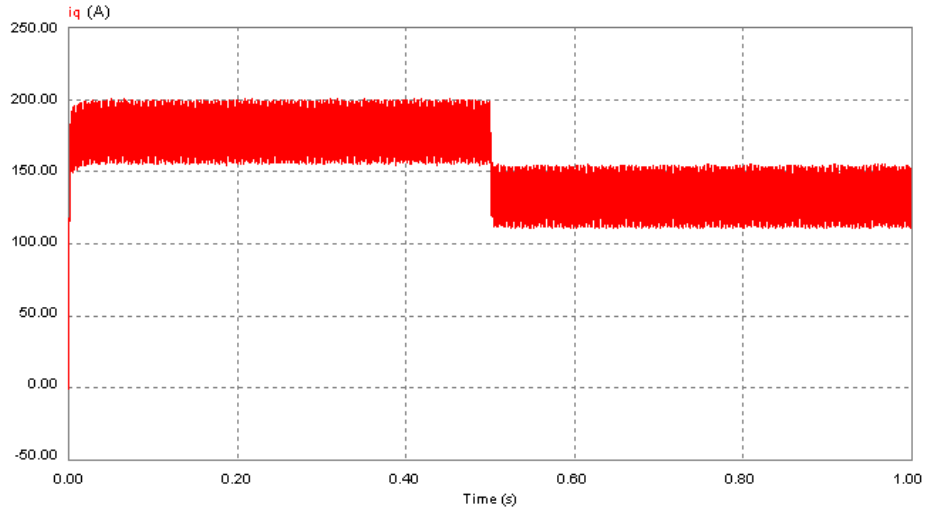

Figure 5.2 i_q response to the change of i_q* from 178A to 134A using pole assignment

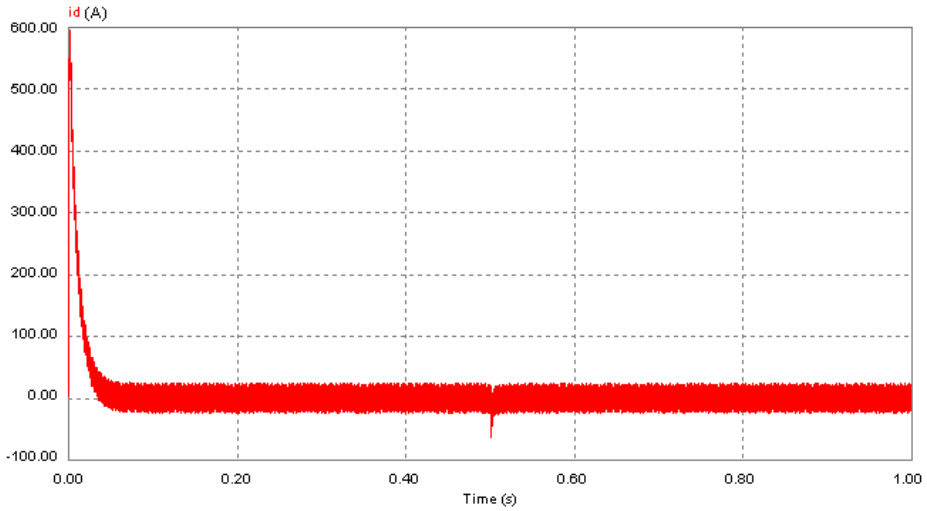

Figure 5.3 i_d response to the change of i_q* from 178A to 134A using pole assignment

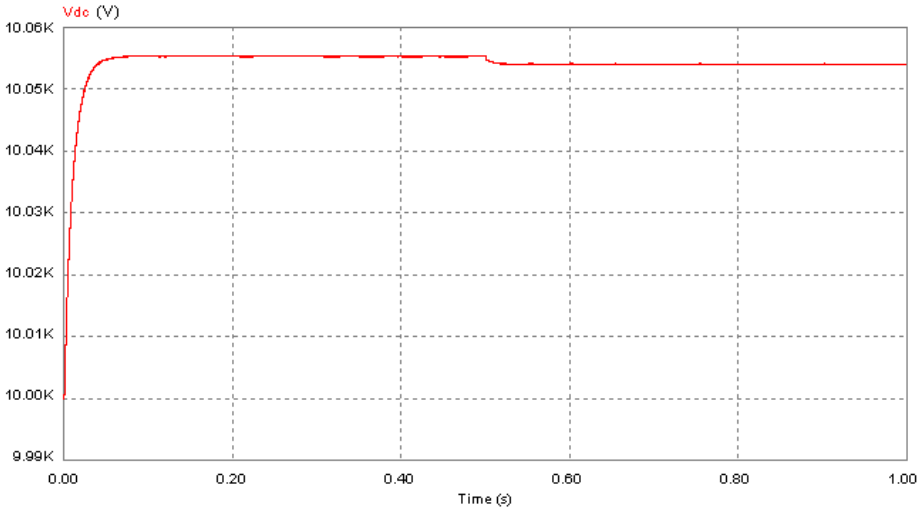

Figure 5.4 V_{dc} response to the change of i_q* from 178A to 134A using pole assignment

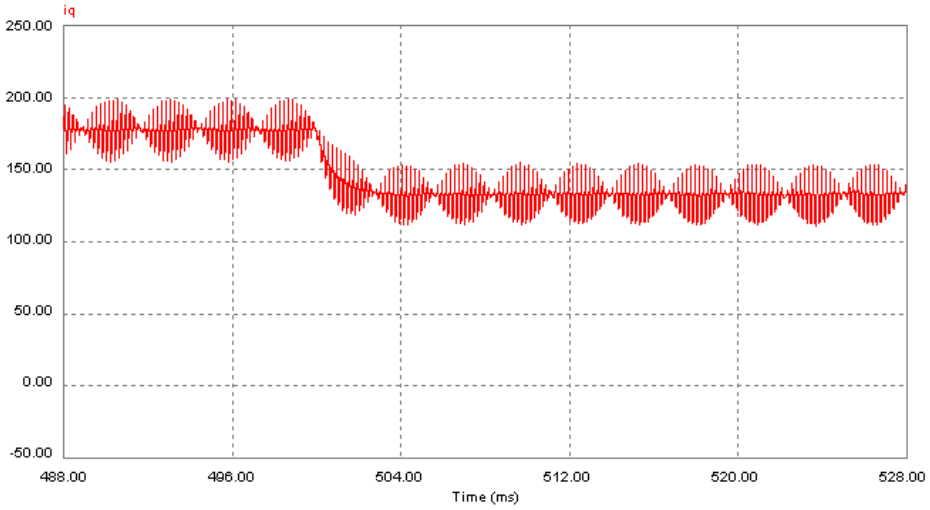

Figure 5.5 Zoom in plot of i_q response to the change of i_q* from 178A to 134A using pole assignment

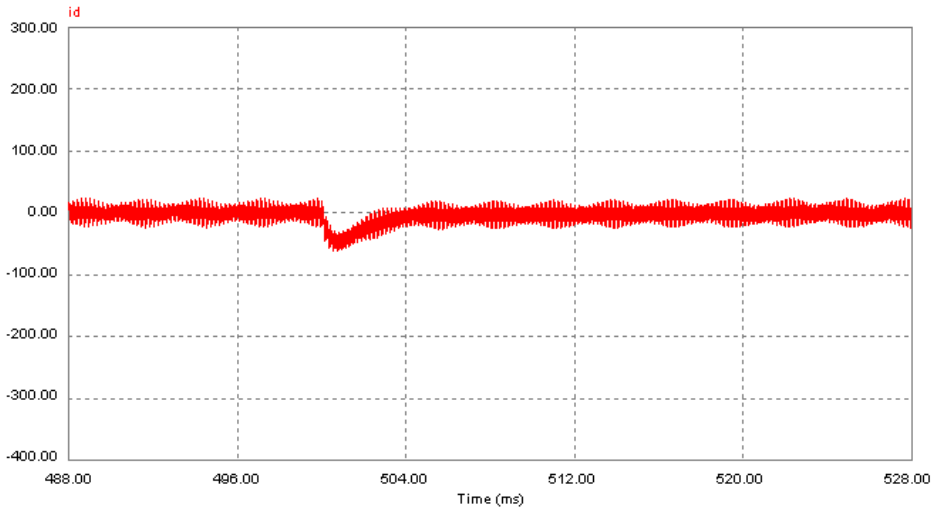

Figure 5.6 Zoom in plot of i_d response to the change of i_q* from 178A to 134A using pole assignment

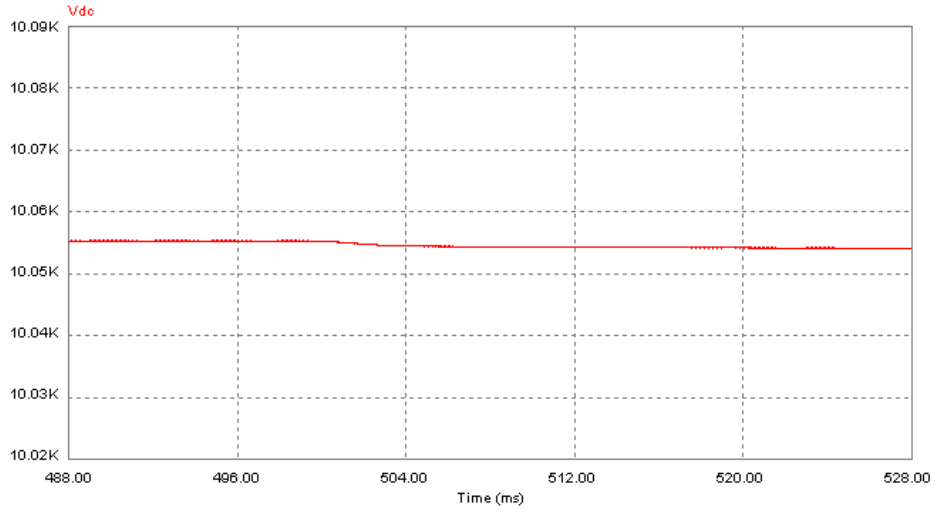

Figure 5.7 Zoom in plot of V_{dc} response to the change of i_q* from 178A to 134A using pole assignment

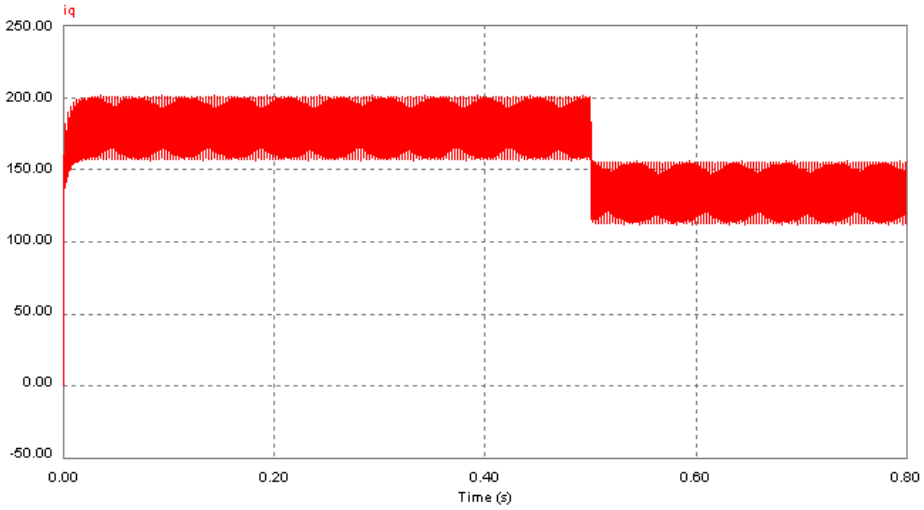

Figure 5.8 i_q response to the change of i_q* from 178A to 134A using LQR controller

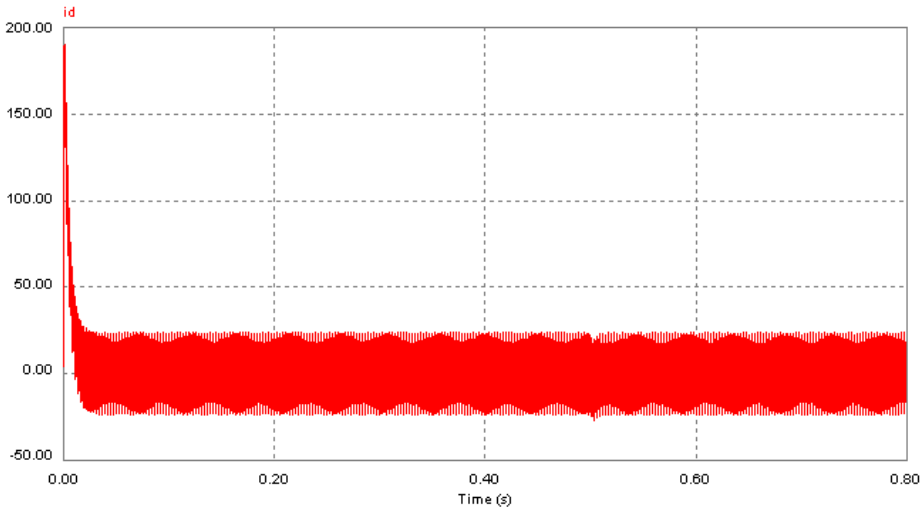

Figure 5.9 i_d response to the change of i_q* from 178A to 134A using LQR controller

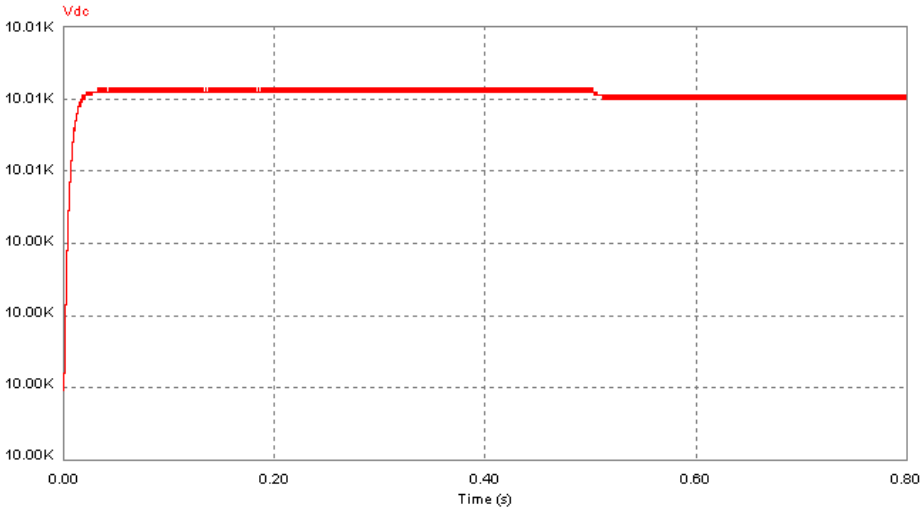

Figure 5.10 V_{dc} response to the change of i_q* from 178A to 134A using LQR controller

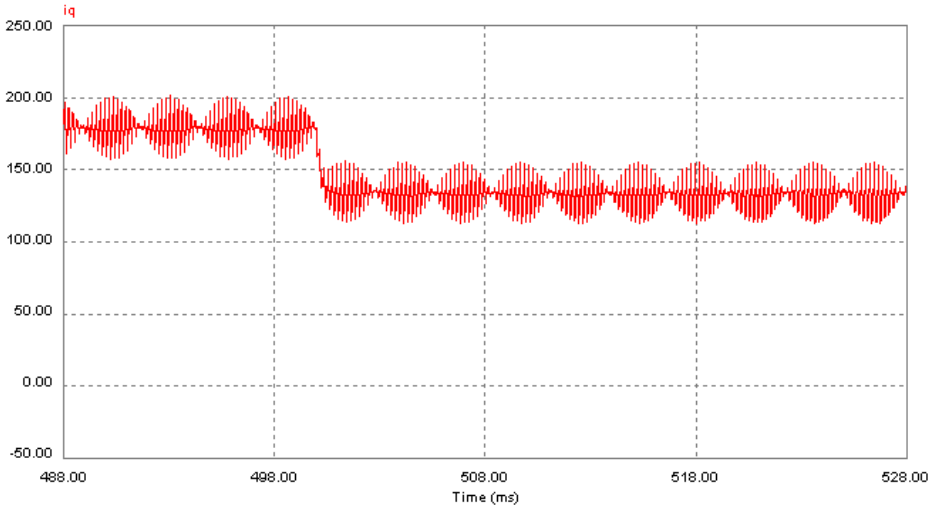

Figure 5.11 Zoom in plot of i_q response to the change of i_q* from 178A to 134A using LQR controller

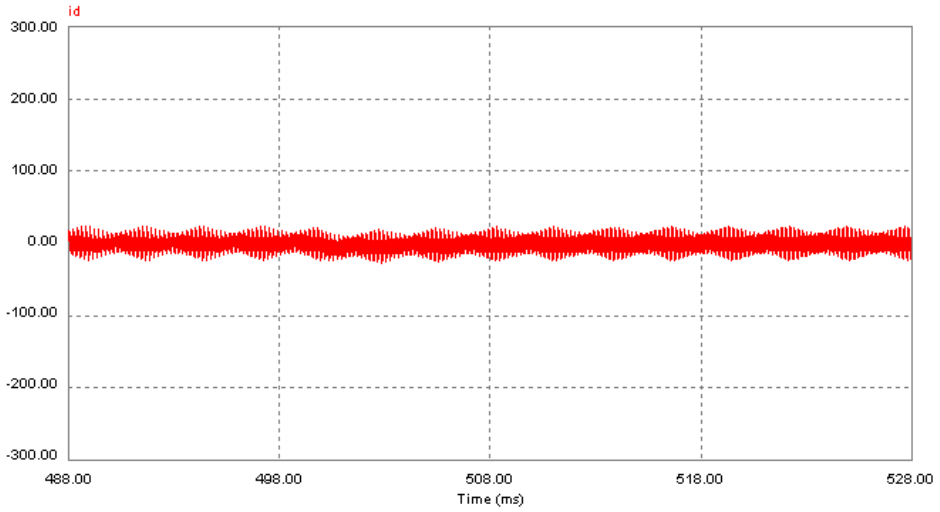

Figure 5.12 Zoom in plot of i_d response to the change of i_q* from 178A to 134A using LQR controller

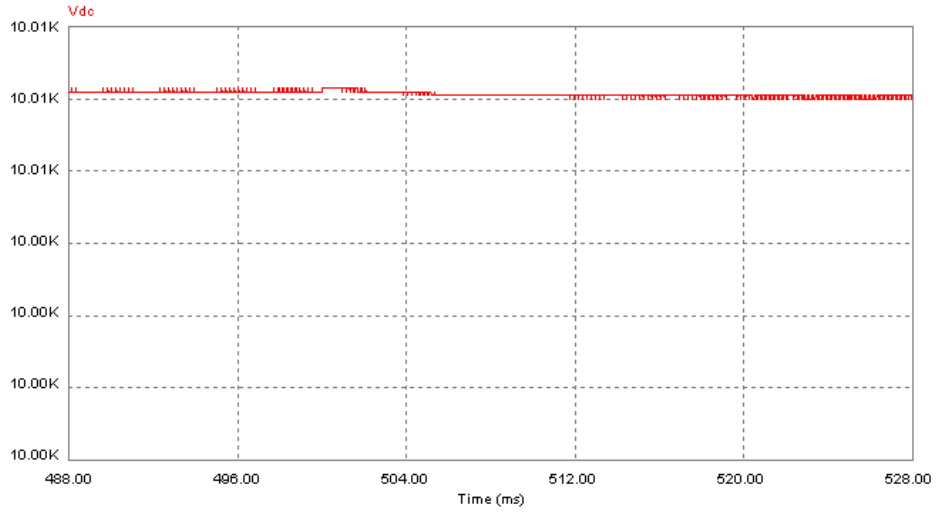

Figure 5.13 Zoom in plot of V_{dc} response to the change of i_q* from 178A to 134A using LQR controller

CONCLUSION

We investigated the dynamic model of a typical STATCOM. Its characteristics show that STATCOM is a nonlinear MIMO system with a control effort saturation requirement. A linearization method can be used to deal with the nonlinear characteristic, if given knowledge of operating point.

Based on the linearized mathematic model of STATCOM, full state feedback controller was designed. The circuit validation showed that this control method is effective and robust.

Two kinds of full state feedback controller (pole assignment and LQR) are designed and compared to investigate a more suitable control method for STATCOM. It was found that LQR controllers do not offer significant performance improvement to pole assignment. However, as a design method the determination of state feedback gains are easier to obtain using LQR method.

There are two topics of further interest noted in this thesis. One topic is to exam the stability and controllability for different operating points. Such a study should lead to a general of knowledge of (1) how various operating points affect the domain of attraction of the equilibrium points and (2) how changes in operating points affect the controllability of STATCOM. Another topic is considering the noise and disturbances inherit in STATCOM. Here one may use robust & optimal control methods to determine if improvements can be made in STATCOM performance.

REFERENCES

[1] L.Gyugyi, "Dynamic compensation of ac transmission lines by solid-state synchronous voltage sources." IEEE Trans. Power Delivery, vol. 9, no. 2 pp.904-911, April 1994.

[2] S. Mori et al., "Development of a large static var generator using self-commutated inverters for improving power system stability." IEEE Trans. Power System, vol. 8, no. 1, Feb. 1993.

[3] Schauder, C.; Gernhardt, M.; Stacey, E.; Lemak, T.; Gyugyi, L.; Cease, T.W.; Edris, A.; "Development of a ±100 MVAr static condenser for voltage control of transmission systems. " IEEE Trans. Power Delivery, Vol. 10, Issue. 3, pp 1486 -1496, July 1995

[4] C. Schauder, M. Gernhardt and E. Stacey et al., "Operation of ±100 MVAR TVA STATCON." IEEE Trans. Power Delivery, vol. 12 , no. 1, Oct. 1997.

[5] John G. Vlachogiannis, "FACTS applications in load flow studies effect on the steady state analysis of the Hellenic transmission system", Electric Power Systems Research, Vol. 55, Issue 3, Sept. 2000.

[6] Papic, I.; Zunko, P.; Povh, D.; Weinhold, M. "Basic control of unified power flow controller ." IEEE Trans. on Power Systems, Vol.12, Issue.4, pp.1734 -1739 Nov. 1997

[7] FACTS & Definitions Task Force of the FACTS Working Group of the DC and FACTS Subcommittee, "Proposed terms and definitions for flexible AC transmission system." IEEE Trans. Power Delivery, vol. 12 , no. 1, Oct. 1997.

[8] Rao, P.; Crow, M.L.; Yang, Z. "STATCOM control for power system voltage control applications." IEEE Trans on Power Delivery, Vol. 15 Issue: 4 , Oct. 2000

[9] Zhuang, Y.; Menzies, R.W.; Nayak, O.B.; Turanli, H.M, "Dynamic performance of a STATCON at an HVDC inverter feeding a very weak AC system." IEEE Trans. on Power Delivery, Vol. 11 Issue: 2, pp.958 -964 April 1996

[10] Sensarma, P.S.; Padiyar, K.R.; Ramanarayanan, V.; "Analysis and performance evaluation of a distribution STATCOM for compensating voltage fluctuations." IEEE Trans. on Power Delivery, Vol. 16 Issue: 2 , pp.259 -264 April 2001

[11] Arabi and P. Kundur, "Power oscillation damping control strategies for FACTS devices using locally measurable quantities". IEEE Trans. on Power Systems. Vol. 10, Issue. 3, Aug.1995.

[12] Garica-Gonzalez, P.; Garcia-Cerrada, "Control system for a PWM-based STATCOM." IEEE Trans. on Power Delivery. Vol. 15 Issue. 4, Oct. 2000.

[13] Arabi, S.; Hamadanizadeh, H.; Fardanesh, B.B. " Convertible static compensator performance studies on the NY state transmission system." IEEE Trans. on Power systems, Vol. 17, Issue: 3 , Aug. 2002

[14] K. R. Padiyar and K. Uma Rao, "Modeling and control of unified power flow controller for transient stability." International Journal of Electrical Power & Energy Systems, Vol.21, Issue 1, January 1999.

[15] Dong Shen; Lehn, P.W, " Modeling, analysis, and control of a current source inverter-based STATCOM." IEEE Trans on Power Delivery, Vol. 17, Issue: 1, pp. 266 -272 , Jan. 2002

[16] Anaya-Lara, O.; Acha, E, "Modeling and analysis of custom power systems by PSCAD/EMTDC ." IEEE Trans on Power Delivery, Vol. 17, Issue. 1, pp. 266 -272 Jan. 2002

[17] Lehn, P.W. "Exact modeling of the voltage source converter ." IEEE Trans. on Power Delivery, Vol. 17, Issue. 1, pp. 217 -222, Jan. 2002

[18] Fujita, H.; Tominaga, S.; Akagi, H. "Analysis and design of a DC voltage-controlled static VAr compensator using quad-series voltage-source inverters ." IEEE Trans. on Industry Applications, Vol. 32, Issue. 4, July-Aug. 1996

[19] Moran, L.T.; Ziogas, P.D. " Joos, G.; Analysis and design of a novel 3-φ solid-state power factor compensator and harmonic suppressor system." IEEE Trans. on Industry Applications, Vol. 25, Issue. 4, July-Aug. 1989

[20] N.Mohan, T. M. Undeland, and W.F. Robbins, Power Electronics: Converters, Applications and Design. New York: Wiley, 1989.

[21] F. Lewis, Applied LQR and Estimation. Prentice hall, 1992.

[22] G. Frankin, J, Powell, and M. Workman, Digital Control of Dynamic System. MA: Addison-Wesley, 1990.

[23] P. C. Krause, Analysis of Electric Machinery. NY: McGraw-Hill Inc., 1986

BIOGRAPHICAL SKETCH

The author was born in China. He received his B.S. degree and M.S. degree in Engineering from Huazhong University of Science & Technology, China.

In the summer of 2001, the author enrolled at Florida State University. His research centered on the modeling and control of FACT devices & system.

The author is a student member of IEEE.